The Astronomical Journal, 135:1968–1981, 2008 May doi:10.1088/0004-6256/135/5/1968
© 2008. The American Astronomical Society. All rights reserved. Printed in the U.S.A.

WEIGHING THE BLACK HOLES IN $z \approx 2$ SUBMILLIMETER-EMITTING GALAXIES HOSTING ACTIVE GALACTIC NUCLEI

D. M. Alexander[1], W. N. Brandt[2], I. Smail[3], A. M. Swinbank[3], F. E. Bauer[4], A. W. Blain[5], S. C. Chapman[6], K. E. K. Coppin[3], R. J. Ivison[7,8], and K. Menéndez-Delmestre[5]

[1] Department of Physics, Durham University, Durham DH1 3LE, UK
[2] Department of Astronomy and Astrophysics, Pennsylvania State University, 525 Davey Laboratory, University Park, PA 16802, USA
[3] Institute for Computational Cosmology, Durham University, South Road, Durham DH1 3LE, UK
[4] Chandra Fellow, Columbia University, 550 W. 112th Street, New York, NY 10027, USA
[5] California Institute of Technology, Pasadena, CA 91125, USA
[6] Institute of Astronomy, Madingley Road, Cambridge CB3 0HA, UK
[7] Astronomy Technology Centre, Royal Observatory, Blackford Hill, Edinburgh EH9 3HJ, UK
[8] Institute for Astronomy, University of Edinburgh, Blackford Hill, Edinburgh EH9 3HJ, UK

Received 2007 June 25; accepted 2008 February 29; published 2008 April 11

ABSTRACT

We place direct observational constraints on the black-hole masses ($M_{\rm BH}$) of the cosmologically important $z \approx 2$ submillimeter-emitting galaxy (SMG; $f_{850\,\mu{\rm m}} \gtrsim 4$ mJy) population, and use measured host-galaxy masses to explore their evolutionary status. We employ the well-established virial black-hole mass estimator to "weigh" the black holes of a sample of $z \approx 2$ SMGs which exhibit broad Hα or Hβ emission. We find that the average black-hole mass and Eddington ratio ($\eta = L_{\rm bol}/L_{\rm Edd}$) of the lower-luminosity broad-line SMGs ($L_{\rm X} \approx 10^{44}$ erg s^{-1}) are $\log(M_{\rm BH}/M_{\odot}) \approx 8.0$ and $\eta \approx 0.2$, respectively; by comparison, X-ray-luminous broad-line SMGs ($L_{\rm X} \approx 10^{45}$ erg s^{-1}) have $\log(M_{\rm BH}/M_{\odot}) \approx 8.4$ and $\eta \approx 0.6$. The lower-luminosity broad-line SMGs lie in the same location of the $L_{\rm X}$–$L_{\rm FIR}$ plane as more typical SMGs hosting X-ray-obscured active galactic nuclei and may be intrinsically similar systems, but orientated so that the rest-frame optical nucleus is visible. Under this hypothesis, we conclude that SMGs host black holes with $\log(M_{\rm BH}/M_{\odot}) \approx 7.8$; we find supporting evidence from observations of local ultra-luminous infrared galaxies. Combining these black-hole mass constraints with measured host-galaxy masses, we find that the black holes in SMGs are $\gtrsim$3 times smaller than those found in comparably massive normal galaxies in the local universe, albeit with considerable uncertainty, and $\gtrsim$10 times smaller than those predicted for $z \approx 2$ luminous quasars and radio galaxies. These results imply that the growth of the black hole lags that of the host galaxy in SMGs, in stark contrast with that previously suggested for radio galaxies and luminous quasars at $z \approx 2$. On the basis of current host-galaxy mass constraints, we show that SMGs and their descendants cannot lie significantly above the locally defined $M_{\rm BH}$–$M_{\rm GAL}$ relationship. We argue that the black holes in the $z \approx 0$ descendents of SMGs will have $\log(M_{\rm BH}/M_{\odot}) \approx 8.6$, indicating that they only need to grow by a factor of $\approx$6 by the present day. We show that this amount of black-hole growth can be achieved within current estimates for the submillimeter-bright lifetime of SMGs, provided that the black holes can grow at rates close to the Eddington limit.

Key words: galaxies: active – galaxies: evolution – infrared: galaxies – X-rays: galaxies

Online-only material: color figures

1. INTRODUCTION

One of the most outstanding astronomical discoveries of the last decade is the finding that every nearby massive galaxy harbors a central black hole with a mass directly proportional to that of the galaxy spheroid (e.g., Magorrian et al. 1998; Ferrarese & Merritt 2000; Gebhardt et al. 2000; Tremaine et al. 2002; Marconi & Hunt 2003; Häring & Rix 2004). This landmark result implies that all massive galaxies have hosted active galactic nucleus (AGN) activity over the past $\approx$13 Gyrs (e.g., Soltan 1982; Yu & Tremaine 2002; Marconi et al. 2004) and suggests that galaxies and their black holes might have grown concordantly, despite nine orders of magnitude difference in size scale (e.g., Silk & Rees 1998; Fabian 1999; King 2003; Wyithe & Loeb 2003; Di Matteo et al. 2005; Bower et al. 2006; Croton 2006; Hopkins et al. 2006b).

Constraining the relative growth of the black hole and spheroid in the high-redshift progenitors of today's massive galaxies remains a fundamental goal of cosmology which can shed light on the connection between AGN activity and star formation, and constrain galaxy-formation models. A number of studies have searched for evolution in the black-hole–spheroid mass relationship at $z \gtrsim 0.5$ by "weighing" the black holes and host galaxies of luminous AGN populations such as quasars and radio galaxies (e.g., Shields et al. 2003, 2006; Treu et al. 2004, 2007; Adelberger & Steidel 2005; McLure et al. 2006; Peng et al. 2006). These studies have typically concluded that the host galaxies of massive black holes ($\gtrsim 10^8\ M_{\odot}$) at $z \approx 2$ were up to $\approx$6 times less massive than those found for comparably massive black holes in the local universe, suggesting that the black hole may grow before the host galaxy. However, by focusing on luminous AGNs, these studies are biased toward selecting the most massive and rapidly growing black holes and could be biased toward evolved extragalactic source populations (e.g., Lauer et al. 2007). These studies may therefore miss the early growth phase of today's massive galaxies where the black-hole–spheroid mass ratio may be different. This is an important consideration when attempting to model and understand how black holes and their host galaxies grow.

Arguably, the best candidates for studying the early growth phase of today's massive galaxies are submillimeter-emitting galaxies (SMGs), such as those identified in deep SCUBA

surveys (e.g., Smail et al. 1997, 2002; Barger et al. 1998; Hughes et al. 1998; Scott et al. 2002; Webb et al. 2003; Borys et al. 2003; Coppin et al. 2006). After intensive multi-wavelength follow-up observations, it is clear that bright SMGs ($f_{850\,\mu m} \gtrsim 4$ mJy) are ultra-luminous ($\gtrsim 10^{12}$ $L_\odot$), gas-rich, massive galaxies at $z \approx 2$ that are undergoing intense bursts of star formation (e.g., Swinbank et al. 2004, 2006; Chapman et al. 2005; Greve et al. 2005; Hainline et al. 2006; Kovács et al. 2006; Tacconi et al. 2006); their star-formation rates are large enough to form a massive galaxy of 10^{11} $M_\odot$ in just (1–2) $\times$ 10^8 yrs. The catalyst for this intense activity is probably galaxy major mergers (e.g., Smail et al. 1998; Chapman et al. 2003; Conselice et al. 2003), which are predicted by hydrodynamical simulations to provide an effective mechanism to transport material toward the central region of the galaxy and trigger nuclear star-formation and AGN activity (e.g., Di Matteo et al. 2005; Springel et al. 2005).

Ultra-deep *Chandra* observations (the 2 Ms *Chandra* Deep-Field-North survey; Alexander et al. 2003a) have shown that at least ≈28–50% of the bright SMG population host heavily obscured AGNs (e.g., Alexander et al. 2003b, 2005a, 2005c), implying joint growth of the galaxy and black hole (see also Ivison et al. 2002; Wang et al. 2004; Pope et al. 2006).[9] The energetics of the AGNs measured at X-ray and mid-infrared (mid-IR) wavelengths are (typically) too low to explain the huge bolometric output of these objects ($L_{\rm bol} \approx 10^{12}$–$10^{13}$ $L_\odot$; e.g., Ivison et al. 2004; Alexander et al. 2003b, 2005a; Lutz et al. 2005), which appears to be dominated by star-formation processes (as shown by the strong star-formation signatures in the mid-IR spectra; e.g., Menéndez-Delmestre et al. 2007; Valiante et al. 2007; Pope et al. 2008).[10] However, the large AGN fraction implies that the black holes are growing almost continuously throughout periods of vigorous star formation. This continuous black-hole growth suggests an abundance of available fuel, and hints that the accretion may be occurring at the Eddington limit (i.e., exponential black-hole growth; e.g., Rees 1984). Although hypothetical, this picture is in good agreement with models for the growth of black holes in SMG-like systems (e.g., Archibald et al. 2002; Di Matteo et al. 2005; King 2005; Granato et al. 2006; c.f., Chakrabarti et al. 2008).

Utilizing deep rest-frame ultraviolet (UV)–near-IR observations, Borys et al. (2005) estimated the stellar masses of the X-ray obscured SMGs identified in Alexander et al. (2005c). They suggested that the Eddington-limited black-hole masses of these objects ($M_{\rm BH,Edd} \approx 10^7$ $M_\odot$) are ≈50 times smaller than the black holes hosted by comparably massive normal galaxies ($M_{\rm GAL} \approx 2.5 \times 10^{11}$ $M_\odot$) in the local Universe. This result suggests that either (1) the growth of the black hole lags that of the host galaxy in SMGs, or (2) the black holes in SMGs are accreting at sub-Eddington rates. The former is in stark contrast with the growth of black holes determined for high-redshift quasars and radio galaxies (e.g., McLure et al. 2006; Peng et al. 2006) while the latter is in conflict with that predicted by most models for the growth of SMG-like systems with an abundance of available fuel (e.g., Archibald et al. 2002; Granato et al. 2006). More direct constraints on the masses and Eddington ratios ($\eta = L_{\rm bol}/L_{\rm Edd}$; i.e., the fraction of the Eddington limit) of the black holes in SMGs are required to distinguish between these different scenarios. These results can then be used to place constraints on the relative black-hole–galaxy growth of this key high-redshift population, including relating SMGs to other high-redshift populations such as quasars and radio galaxies.

In this paper, we employ the well-established virial black-hole mass estimator (e.g., Wandel et al. 1999; Kaspi et al. 2000) to directly determine black-hole masses ($M_{\rm BH}$) and η for the small subset of SMGs that have broad emission lines. The virial black-hole mass estimator provides the most direct and accessible method currently available to determine black-hole masses at high redshift, and this is the first study that has used this technique to estimate $M_{\rm BH}$ for the cosmologically important SMG population. We use these results to estimate the black-hole properties of the X-ray-obscured SMGs identified in Alexander et al. (2005a, 2005c). Observations of nearby ultra-luminous IR Galaxies ($L_{\rm IR} \gtrsim 10^{12}$ $L_\odot$; ULIRGs; e.g., Sanders & Mirabel 1996) hosting obscured AGNs are also used to determine the Eddington ratios and intrinsic AGN properties of these $z \approx 0$ analogs to the X-ray-obscured SMG population and, by inference, place indirect constraints on the properties of typical SMGs. We have adopted $H_0 = 71$ km s^{-1} Mpc^{-1}, $\Omega_{\rm M} = 0.27$, and $\Omega_\Lambda = 0.73$ throughout.

2. SAMPLES AND METHOD

2.1. Samples

We have defined several samples to use in this study, which we briefly describe below. We have used two SMG samples, a broad-line SMG sample, to enable us to directly estimate $M_{\rm BH}$ and η, and an X-ray-obscured SMG sample, which is more representative of the overall SMG population than the broad-line SMG sample. The broad-line SMG sample is further broken down into "lower-luminosity broad-line SMGs," which includes objects with $L_{\rm X} \approx 10^{44}$ erg s^{-1}, and "X-ray-luminous broad-line SMGs," which includes objects with $L_{\rm X} \approx 10^{45}$ erg s^{-1}; see Section 3.1 for details of the sample selection. For the X-ray-obscured SMG sample we focus on the $z > 1.8$ SMGs that host X-ray identified AGNs in Alexander et al. (2005a, 2005c), to probe the peak epoch of SMG activity (e.g., $z \approx 2.2$; Chapman et al. 2005); we thus removed three $z \lesssim 1$ SMGs, which make up the low-redshift tail of the SMG population. The average redshift of the $z > 1.8$ X-ray-obscured SMG sample ($z = 2.29 \pm 0.32$) is consistent with that of the broad-line SMG sample ($z = 2.36 \pm 0.26$).

We have also defined two samples of nearby ULIRGs to provide more direct insight into the black-hole masses and AGNs of dust-obscured objects with similar bolometric luminosities to the SMG population. The first sample comprises ULIRGs hosting obscured AGN activity for which we were able to estimate $M_{\rm BH}$ and η from the presence of broad near-IR emission lines; see Section 4.1 for details of the sample selection. The second sample is distance limited and comprises all of the ULIRGs hosting AGN activity that lie within 200 Mpc. The X-ray and far-IR data of this sample is used to assess whether the intrinsic properties of the AGNs in the X-ray-obscured SMG sample have been underestimated, which would lead to underestimates in $M_{\rm BH}$; see Section 4.2 for details of the sample selection.

2.2. Method

Black-hole masses have been directly measured from the velocity dispersion of stars/gas in the nuclear regions of galaxies in the local Universe (e.g., Kormendy & Richstone 1995; Sarzi et al. 2001; Gebhardt et al. 2003; Pinkney et al. 2003). Black

[9] The sensitivity of instruments prevents good statistics on the prevalence of AGN activity in the faint SMG population ($f_{850\,\mu m} \lesssim 4$ mJy).

[10] We note that in this respect SMGs are unlike the local ultra-luminous infrared galaxy (ULIRG) Arp 220, which has ambiguous AGN and star-formation signatures (e.g., Haas et al. 2001; Downes & Eckart 2007).

holes cannot be "weighed" using the same techniques at high redshift due to poorer spatial resolution and lower signal-to-noise ratio data. However, the well-established virial black-hole mass estimator, which works on the assumption that the broad-line region (BLR) in AGNs is under the gravitational influence of the black hole (i.e., $V^2 = GM/r$; see Peterson & Wandel 1999, 2000 for evidence), provides an apparently reliable, if indirect, measurement of $M_{\rm BH}$ for more distant AGNs (e.g., Wandel et al. 1999; Kaspi et al. 2000; McLure & Dunlop 2002; Vestergaard 2002; Peterson et al. 2004; Vestergaard & Peterson 2006). Using this technique, the masses of black holes in quasars up to $z \approx 6.4$ have been estimated (e.g., Willott et al. 2003; McLure & Dunlop 2004; Vestergaard 2004). The calibration of this technique is predominantly restricted to reverberation mapping of nearby AGNs in the local universe; however, the first reverberation mapping experiments at high redshift are already underway (see Kaspi 2007; Kaspi et al. 2007).

The primary aim of this paper is to estimate $M_{\rm BH}$ for the X-ray-obscured SMG sample to determine the relative black-hole–galaxy growth of SMGs and explore their evolutionary status. The X-ray-obscured SMGs already have host-galaxy mass constraints (e.g., Borys et al. 2005), and since ≈28–50% of SMGs host heavily obscured AGNs they should be representative of the SMG population. However, the presence of heavy absorption in these SMGs hides the BLR in the majority of these systems (e.g., Swinbank et al. 2004; Alexander et al. 2005a; Chapman et al. 2005), making it difficult to directly use the virial black-hole mass estimator to determine their black-hole properties. Fortunately, the identification of broad emission lines from a small number of SMGs (e.g., Swinbank et al. 2004; Takata et al. 2006) provides the opportunity to estimate the black-hole masses and Eddington ratios for this subset of the SMG population, providing a lever to determine constraints for the, more typical, X-ray-obscured SMGs. For example, taking the canonical approach that the relationship between broad-line AGNs and obscured AGNs is the orientation of an optically and geometrically thick torus (i.e., the unified AGN model; e.g., Antonucci 1993), the average Eddington ratios and black-hole masses of the X-ray-obscured SMGs should be comparable to the broad-line SMGs. In this scenario, we would calculate the black-hole masses of the SMGs as

$$M_{\rm BH(XO\text{-}SMG)} = \frac{M_{\rm BH,Edd(XO\text{-}SMG)}}{\eta_{\rm (BL\text{-}SMG)}}, \quad (1)$$

where $M_{\rm BH(XO\text{-}SMG)}$ and $M_{\rm BH,Edd(XO\text{-}SMG)}$ are the black-hole mass and X-ray-derived Eddington-limited black-hole mass for the X-ray obscured SMGs, and $\eta_{\rm (BL\text{-}SMG)}$ is the Eddington ratio for the broad-line SMGs, which is defined as

$$\eta = \frac{\kappa L_{\rm X}}{L_{\rm Edd}}, \quad (2)$$

where $\kappa_{2-10\,\rm keV}$ is the X-ray-to-bolometric luminosity conversion. Our overall approach is similar in essence to that adopted by McLure et al. (2006) when exploring the black-hole–galaxy mass ratio for radio galaxies. We investigate $M_{\rm BH}$, η, and the black-hole–galaxy mass ratio for the SMGs in Section 3.

However, it is also possible that the relationship between the broad-line SMGs and the X-ray obscured SMGs is not the orientation of an obscuring torus toward the line of sight. For example, the broad-line SMGs might represent a more evolved stage in the evolution of the SMG population or they may be undergoing a period of increased mass accretion that makes the BLR temporarily visible. Since an optically bright broad-line AGN is often considered to be at a later phase in the evolution of massive galaxies than an X-ray-obscured AGN (e.g., Sanders et al. 1988; Granato et al. 2006; Hopkins et al. 2006a; Chakrabarti et al. 2008), in the evolutionary scenario, the black-hole masses of the broad-line SMGs will provide an upper limit to the black-hole masses of the X-ray-obscured SMGs. By comparison, in the increased mass accretion scenario, the black-hole masses of the X-ray-obscured SMGs would be the same as the broad-line SMGs but the Eddington ratios would be lower. Unless we can rule out these alternative scenarios, our determination of $M_{\rm BH}$ for the X-ray-obscured SMGs will be subject to larger uncertainties. However, although the presence of absorption in the X-ray-obscured SMGs hinders direct black-hole mass measurements, the identification of broad Paα in a small number of nearby obscured ULIRGs provides the potential to gain insight into the Eddington ratios for obscured AGNs similar to those found in the X-ray-obscured SMGs (Veilleux et al. 1997, 1999), and hence distinguish between these different scenarios. The broad Paα emission from these obscured ULIRGs is thought to be observed through the atmosphere of a dusty obscuring torus, which is assumed to be optically thin at near-IR wavelengths. The similarity between the bolometric luminosities, spectral energy distributions (SEDs), and morphological properties of SMGs and nearby ULIRGs suggests that distant SMGs may be "scaled-up" versions of ULIRGs, providing validation for this approach (e.g., mid-IR spectra; Menéndez-Delmestre et al. 2007; Valiante et al. 2007; submillimeter (submm) dust/gas emission and extent, Greve et al. 2005, 2006; see Table 2 in Tacconi et al. 2006; major mergers, Chapman et al. 2003; Conselice et al. 2003). We determine $M_{\rm BH}$, η, and the black-hole–galaxy mass ratio for the nearby ULIRGs in Section 4.

3. WEIGHING THE BLACK HOLES OF $z \approx 2$ SMGs HOSTING AGN ACTIVITY

In this section, we determine $M_{\rm BH}$ for the broad-line SMGs using the virial black-hole mass estimator of Greene & Ho (2005), which calculates black-hole masses solely from the properties of the Hα or Hβ emission line, and reduces potential uncertainties on the luminosity of the AGN (e.g., contaminating emission from the host galaxy or an accretion-related jet) when compared to other estimators. We estimate Eddington ratios for these sources using the black-hole mass and the X-ray luminosity, as a proxy for the mass accretion rate. We then compare the properties of the X-ray-obscured SMGs to the broad-line SMGs and use these results to constrain $M_{\rm BH}$ and the black-hole–galaxy mass ratio for the more typical X-ray-obscured SMGs.

3.1. The Selection of Broad-Line SMGs

The broad-line SMG sample is selected from the redshift survey of SMGs by Chapman et al. (2005), the same original source as the X-ray-obscured SMG sample (Alexander et al. 2005a, 2005c). The initial sample comprises 12 SMGs with broad (FWHM >1000 km s^{-1}) Hα or Hβ emission from Swinbank et al. (2004), Takata et al. (2006), and new Keck NIRSPEC data (K. Menéndez-Delmestre et al., 2008 in preparation). We removed six objects where the [O III]λ5007 emission-line profile was found to be similar to the Hα/Hβ emission-line profile. [O III]λ5007 is a forbidden line that is not intrinsically broad (typically FWHM $\lesssim 600$ km s^{-1}), suggesting

Table 1
Broad-Line SMGs

Name (SMMJ)	z	$\log(L_{H\alpha})$[a] (erg s^{-1})	FWHM$_{H\alpha}$ (km s^{-1})	$\log(M_{BH})$ ($M_\odot$)	$\log(L_X)$[b] (erg s^{-1})	Refs
123635.5+621424	2.015	43.4	1600 ± 200	7.3	43.8	1,2
123716.0+620323	2.053	44.1	2400 ± 500	8.2	44.1	2,3
131215.2+423900	2.555	43.7[c]	2500 ± 500[c]	7.9	44.9	4,5
131222.3+423814	2.560	44.3[c]	2600 ± 1000[c]	8.3	44.7	4,5
163655.8+405914	2.592	44.4	3000 ± 400	8.5	45.0	1,6
163706.5+405313	2.375	43.3	3300 ± 1000	7.9	<44.0	1,6

Notes.
[a] The Hα luminosity has been corrected for extinction, determined from the broad-line Hα/Hβ flux ratio, except for the two 13 h sources for which only Hβ data are available (these two sources are optically bright and probably do not suffer significant extinction; see Section 3.1).
[b] Rest-frame 2–10 keV band, corrected for absorption; see Section 3.3.
[c] Line width is for Hβ. The Hα luminosity is calculated from the Hβ luminosity, assuming an intrinsic Hα/Hβ = 3.1.
References.
(1) Swinbank et al. (2004); (2) Alexander et al. (2003a); (3) K. Menéndez-Delmestre et al., 2008 in preparation; (4) Takata et al. (2006); (5) Mushotzky et al. (2000); (6) Manners et al. (2003).

that the broadening of the Hα/Hβ emission in these six objects might not be intrinsic to the BLR and could, instead, be due to external kinematics (e.g., outflows and multiple components within galaxy mergers; e.g., Heckman et al. 1981; Whittle 1985, 1988). However, before applying the virial black-hole mass estimator to the remaining six objects in the broad-line SMG sample, it is necessary to verify that the BLR emission is not dominated by scattered light (as would be expected if the BLR was completely obscured; e.g., Antonucci & Miller 1985; Young et al. 1996) and to correct the broad-line emission for extinction.

The detection of submm emission from the broad-line SMGs implies the presence of dust, which might obscure the BLR in some cases. To test if the BLR emission is seen directly (rather than in scattered light), we compared the broad-line luminosity to the rest-frame 2–10 keV luminosity; see Table 1 for the source properties. We found that the broad-line SMGs have stronger Hα emission than expected from the local Hα–X-ray luminosity relationship of Ward et al. (1988), indicating that the BLR is brighter than found in typical broad-line AGNs, and demonstrating that the emission is being seen directly. Indeed, the Hα–X-ray luminosity ratios of the broad-line SMGs are similar to those of nearby ULIRGs ($L_X/L_{H\alpha} \approx 3$, a factor $\approx$ 6 higher than the average in Ward et al. 1988; e.g., Imanishi & Terashima 2004).

We estimated the extinction to the BLR for each source on the basis of the broad Hα/Hβ emission-line ratio, following the prescription of Ward et al. (1987) for an intrinsic ratio of Hα/Hβ = 3.1 (i.e., Case B recombination; Osterbrock 1989) and the reddening curve of Calzetti et al. (2000). Extinction corrections are rarely applied to the broad-line luminosities of AGNs used in studies estimating virial black-hole masses, even when rest-frame UV emission lines are used. However, even in our potentially dust-obscured sample of broad-line AGNs, we did not find evidence for large amounts of extinction (the mean extinction correction was $A_V \approx 1.2$ mag). The comparatively low level of extinction suffered by the nucleus when compared to the high extinction suffered by the star-forming regions in SMGs (e.g., Swinbank et al. 2004; Takata et al. 2006) could be due to the dust tracing the extended star-forming regions rather than the nucleus; we note that by selecting broad-line AGNs our sample will also be biased toward objects with low levels of nuclear extinction. The intrinsic broad Hα/Hβ emission-line ratio in many broad-line AGNs is larger than the theoretical Case B limit (e.g., Adams & Weedman 1975; Osterbrock 1977), which would give slightly smaller black-hole masses for our broad-line SMGs.

Two of the broad-line SMGs did not have Hα emission-line constraints; see Table 1. However, since these two objects are the optically brightest $z \approx 2$ SMGs in the Chapman et al. (2005) sample and have rest-frame UV and/or lower-order Balmer broad emission lines in their spectra (Chapman et al. 2005; Takata et al. 2006), the extinction to their BLRs is likely to be small. Furthermore, since the average broad Hα/Hβ emission-line ratio of the AGNs used in the Greene & Ho (2005) virial black-hole mass estimation is larger than the expected intrinsic ratio (the average broad Hα/Hβ ratio of the sample is 3.5), this effectively allows for the inclusion of small amounts of reddening, and hence we adopted zero reddening for these two SMGs.

The basic properties of the broad-line SMG sample are given in Table 1. Although this sample is not complete, it is representative of SMGs spanning a wide range in X-ray luminosity. We make a distinction between the broad-line SMGs studied here and X-ray-selected quasars detected at submm wavelengths (e.g., Page et al. 2001, 2004; Stevens et al. 2005), which have smaller space densities than the SMG populations studied here; however, see Section 5.2 and Coppin et al. (2008) for possible overlap between these source populations.

3.2. Weighing the Black Holes in Broad-Line SMGs

Figure 1 shows the emission-line properties of the broad-line SMG sample. Using the Greene & Ho (2005) virial black-hole mass estimator, the black-hole masses of the broad-line SMG sample are $\log(M_{BH}/M_\odot) \approx 7.3$–$8.5$ and the mean is $\log(M_{BH}/M_\odot) = 8.0 \pm 0.4$. By comparison, optically selected $z \approx 2$ quasars in the Sloan Digital Sky Survey (SDSS) have black-hole masses about an order of magnitude higher ($\log(M_{BH}/M_\odot) = 8.9 \pm 0.3$; see Figure 1 in McLure & Dunlop 2004). This difference is largely due to selection effects as the SDSS quasars are luminous at rest-frame UV wavelengths ($i < 19.1$; Schneider et al. 2003), and are therefore biased

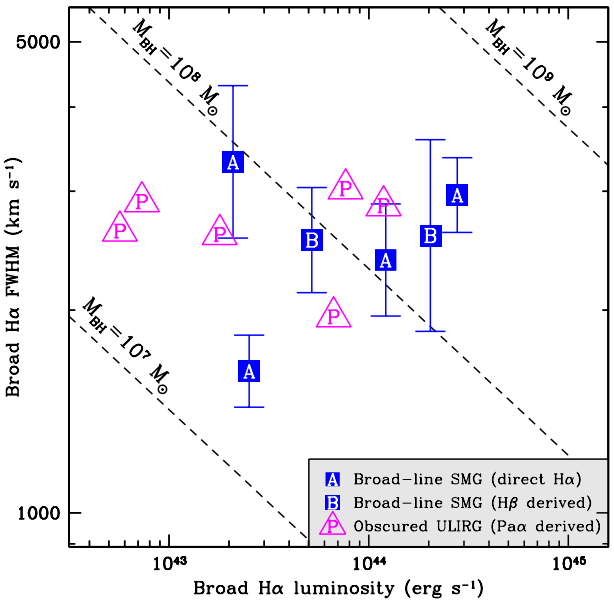

Figure 1. Hα properties of the broad-line SMGs and obscured ULIRGs. Sources indicated with letters have had their Hα properties determined from their extinction-corrected Hα emission ("A"), derived from their Hβ properties for an intrinsic Hα/Hβ ratio of 3.1 ("B"; see Section 3.1), or derived from their Paα properties for an intrinsic Hα/Paα ratio of 8.6 ("P"; see Section 4.1). The dashed lines show the relationship between the black-hole mass (M_{BH}) and the broad Hα emission-line properties on the basis of the virial black-hole mass estimator of Greene & Ho (2005). Taken at face value the data suggest that broad-line SMGs have a range of black-hole masses with a mean of $\log(M_{BH}/M_\odot) \approx 8.0$; the obscured ULIRGs have a mean black-hole mass of $\log(M_{BH}/M_\odot) \approx 7.8$. However, if it is assumed that the BLR gas in the broad-line SMGs is distributed in a disk that is seen close to pole on (rather than the BLR gas being isotropically distributed and in random motion) then the average black-hole mass will be ≈2.7 times larger, on the basis of the model described in the text (see Section 3.2).

(A color version of this figure is available in the online journal)

toward the largest black holes (i.e., rarer objects), while all but two of the broad-line SMGs have $i > 19.1$. However, the comparative narrowness of the broad lines in these SMGs when compared to the typical quasar population (≈2500 km s^{-1} versus ≈5000 km s^{-1}) suggests relatively modest black-hole masses. For comparison, the mean black-hole mass of $z = 1.8$–2.1 SDSS quasars with FWHM < 3500 km s^{-1} is $\log(M_{BH}/M_\odot) = 8.5 \pm 0.2$ (McLure & Dunlop 2004).

The broad-line SMG black-hole mass constraints are calculated for the scenario where the BLR gas is isotropically distributed and in random motion within the gravitational potential of the black hole, as typically assumed. However, if the BLR gas is distributed in a disk which is observed close to pole on then the broad-line width will only provide a lower limit to the intrinsic velocity of the BLR (and hence the black-hole mass; e.g., Jarvis & McLure 2006). Indeed, the narrowness of the broad lines indicates that our broad-line SMG sample may be biased toward objects seen pole on (McLure & Dunlop 2002; Collin et al. 2006; Jarvis & McLure 2006). We can assess the potential effect of a disk-like BLR by assuming that the average inclination angle of the BLR can be calculated from the obscured:unobscured AGN ratio of the SMG population, under the hypothesis of the unified AGN model. On the basis of the X-ray spectral analysis of SMGs by Alexander et al. (2005a), the obscured:unobscured AGN ratio for the SMGs is ≈5–10, giving a maximum BLR inclination for the broad-line SMGs of $i < 25$–$34°$ and an average BLR inclination of $i = 18$–$25°$ (e.g., Equation (1) in Arshakian 2005). Using the BLR model of McLure & Dunlop (2002), the average correction to the black-hole mass for a disk-like BLR would be ≈2.7, giving a mean mass for the broad-line SMG sample of $\log(M_{BH}/M_\odot) = 8.4 \pm 0.4$; see Figure 1 in McLure & Dunlop (2002).[11] There is no conclusive evidence that the BLR is orientated in a disk in radio-quiet AGNs; however, for completeness we conservatively consider both average black-hole masses in these initial analyses.

3.3. The Eddington Ratios of Broad-Line SMGs

The Eddington ratio of a black hole is calculated from the black-hole mass and the mass accretion rate (e.g., Rees 1984) and provides a measurement of the black hole "growth time" (i.e., the time required for the black hole to double in mass); see Equation (2). The determination of accurate Eddington ratios is challenging since they rely upon excellent measurements of the black-hole mass, the bolometric correction, and the conversion between the AGN bolometric luminosity and the mass accretion rate. However, the primary reason that we calculate Eddington ratios in this paper is to provide a way to scale between the measured black-hole masses of the broad-line SMGs and the Eddington-limited black-hole masses of the X-ray-obscured SMGs; see Equation (1). The Eddington ratios derived in this paper should therefore be considered indicative rather than absolute values (as is generally the case for high-redshift studies). An advantage of this approach is that it is only important that the X-ray-to-bolometric luminosity corrections of the broad-line SMGs and the X-ray-obscured SMGs are the same. This assumption seems reasonable given that (1) the broad-line SMGs and the X-ray-obscured SMGs have similar X-ray and far-IR luminosities (see Section 3.4 and Figure 3), and (2) the broad-line SMGs and obscured ULIRGs have similar Eddington ratios (see Section 4).

Here we calculate the Eddington ratio for the broad-line SMGs using the X-ray luminosity as a proxy for the mass accretion rate. We converted the X-ray luminosity to the bolometric AGN luminosity using the Elvis et al. (1994) mean spectral energy distribution ($\kappa_{2-10\,keV} \approx 35$); see Equation (2). We note that using different bolometric conversions (e.g., Marconi et al. 2004; Vasudevan & Fabian 2007) will increase our estimate of the Eddington ratio by up to a factor of ≈2 (up to $\kappa_{2-10\,keV} \approx 70$ for high accretion-rate AGNs). However, adopting different bolometric conversions will not change our determination of the black-hole masses for the X-ray-obscured SMGs; see Equation (3) & Section 3.4. The X-ray luminosities of the six broad-line SMGs were determined using *Chandra* data from Mushotzky et al. (2000), Manners et al. (2003), and Alexander et al. (2003a). When appropriate, X-ray-absorption corrections were made following Alexander et al. (2005a); see Figure 5 and Section 4.2.

In Figure 2, we show the X-ray-derived mass accretion rate versus virial black-hole mass for the broad-line SMG sample; see Section 4.1 for a discussion of the obscured ULIRGs. The most luminous broad-line SMGs have an average Eddington ratio comparable to those of $z = 1.8$–2.1 SDSS quasars with narrow broad lines ($\eta \gtrsim 0.5$; e.g., McLure & Dunlop 2004). However, an estimate of the average Eddington ratio for the broad-line SMG sample depends upon the distribution of the gas in the BLR. If the BLR gas is isotropically distributed

[11] We highlight here the close similarity between the estimated average inclination angle of the BLR and that estimated for the CO emission in the host galaxies of submm-detected quasars ($i \approx 13°$; Carilli & Wang 2006).

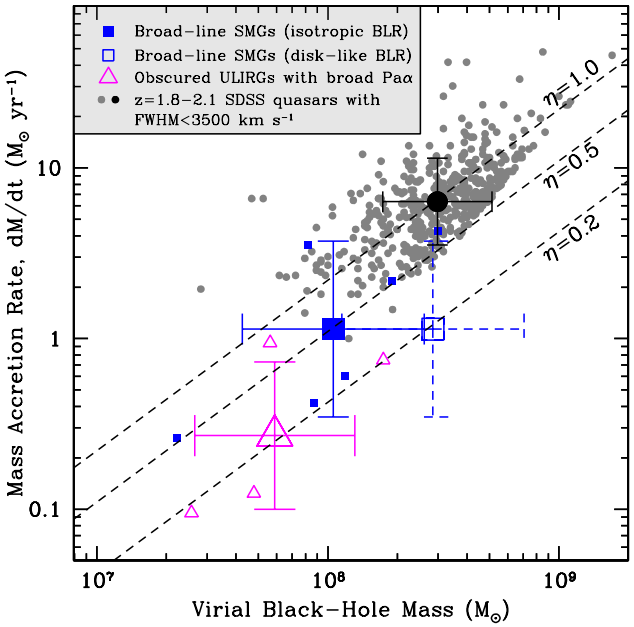

Figure 2. Mass accretion rate versus black-hole mass of the broad-line SMG sample, a sample of nearby ULIRGs hosting obscured AGNs but with detected broad Paα emission, and $z = 1.8$–2.1 SDSS quasars with comparatively narrow emission lines (FWHM < 3500 km s^{-1}; data taken from McLure & Dunlop 2004). The error bars correspond to 1σ uncertainties on the average properties. The dashed lines indicate Eddington ratios ($\eta = L_{\rm bol}/L_{\rm Edd}$; i.e., the fraction of the Eddington limit) of $\eta = 0.2$, $\eta = 0.5$, and $\eta = 1.0$. The average Eddington ratio of the broad-line SMGs is $\eta \approx 0.5$, assuming that the BLR gas is isotropically distributed and in random motion, or $\eta \approx 0.2$, assuming that the BLR gas is distributed in a disk that is observed close to pole on (see Section 3.2); this is compared to the average for the SDSS quasars with comparatively narrow emission lines ($\eta \approx 1.0$ for BLR gas in random motion). The average Eddington ratio of the nearby ULIRGs hosting obscured AGNs, where inclination-angle effects will not be as important, is $\eta \approx 0.2$ (see Section 4.1).

(A color version of this figure is available in the online journal)

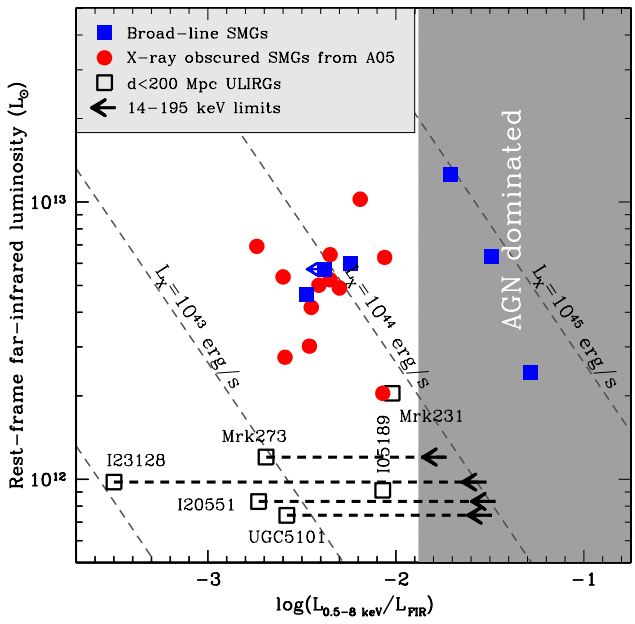

Figure 3. Rest-frame far-IR luminosity versus X-ray-to-far-IR luminosity ratio for the X-ray-obscured SMGs, the broad-line SMGs, and the $d < 200$ Mpc ULIRGs; the X-ray luminosities are corrected for absorption, where necessary. The arrows indicate the 14–195 keV limits for the $d < 200$ Mpc ULIRGs from *Swift*-BAT (Markwardt et al. 2005); both Mrk 231 and I05189-2524 are detected at high X-ray energies (20–50 keV) using *BeppoSAX*-PDS (Dadina 2007). The far-IR luminosities for the X-ray obscured SMG and the broad-line SMGs are calculated from the radio luminosity assuming the radio-to-far-IR relationship (the former are taken from Alexander et al. 2005a), and the far-IR luminosities for the $d < 200$ Mpc ULIRGs are taken from Sanders et al. (2003). The diagonal dashed lines indicate different X-ray luminosities and the shaded region shows where AGN-dominated sources will lie on the basis of the Elvis et al. (1994) spectral energy distribution (taken from Figure 8 of Alexander et al. 2005a). The three lower-luminosity broad-line SMGs lie in the same location of the $L_{\rm X}$–$L_{\rm FIR}$ plane as the X-ray-obscured SMGs, however, the other three broad-line SMGs have X-ray luminosities $\approx$10 times higher than the broad-line SMGs and are not typical of the SMG population (these X-ray-luminous broad-line SMGs are probably AGN-dominated systems).

(A color version of this figure is available in the online journal)

and in random motion, as typically assumed, then the average Eddington ratio is $\eta = 0.5^{+1.0}_{-0.3}$, while the average Eddington ratio drops to $\eta = 0.2^{+0.4}_{-0.1}$ if the BLR gas is distributed in a disk that is observed close to pole on. The higher value is consistent with Eddington-limited accretion while the lower value is similar to those found for the distant broad-line AGN population (e.g., McLure & Dunlop 2004; Kollmeier et al. 2006) and would appear to suggest that broad-line SMGs are not growing their black holes at a significantly faster rate than typical submm-undetected broad-line AGNs (only $\approx$5–15% of $z \approx 2$ quasars are submm detected; Priddey et al. 2003; Page et al. 2004).

3.4. The Black-Hole Masses of the X-Ray Obscured SMGs

Due to the presence of heavy obscuration in the majority of the SMG population, we are unable to use the virial black-hole mass estimator to constrain directly the black-hole masses of the X-ray-obscured SMGs. However, if the X-ray-obscured SMGs are related to the broad-line SMGs either via the orientation of an obscuring torus (e.g., Antonucci 1993) or in terms of an evolutionary scenario (e.g., Sanders et al. 1988), then we can use the black-hole masses and Eddington ratios of the broad-line SMGs to constrain the black-hole masses of the X-ray-obscured SMGs; see Section 2 for a discussion of these scenarios.

For example, applying the Eddington ratios of the broad-line SMGs ($\eta = 0.2$–0.5) to the average Eddington-limited black-hole mass of the $z > 1.8$ X-ray obscured SMG sample ($\log(M_{\rm BH,Edd}/M_\odot) \approx 7.1$; Alexander et al. 2005c) gives $\log(M_{\rm BH}/M_\odot) \approx 7.4$–7.8; see Equation (1). These average black-hole masses are $\approx$4 times smaller than those estimated for the broad-line SMGs, which is due to the difference in average X-ray luminosity between the X-ray obscured SMGs and the broad-line SMGs (mean 0.5–8.0 keV luminosities of $\approx 8 \times 10^{43}$ erg s^{-1} and $\approx 3 \times 10^{44}$ erg s^{-1}, respectively); i.e.

$$M_{\rm BH(XO\text{-}SMG)} = \frac{L_{\rm X(XO\text{-}SMG)}}{L_{\rm X(BL-SMG)}} M_{\rm BH(BL\text{-}SMG)}, \quad (3)$$

where $M_{\rm BH(XO\text{-}SMG)}$ and $L_{\rm X(XO\text{-}SMG)}$ are the black-hole mass and X-ray luminosity of the X-ray-obscured SMGs, and $M_{\rm BH(BL\text{-}SMG)}$ and $L_{\rm X(BL\text{-}SMG)}$ are the black-hole mass and X-ray luminosity of the broad-line SMGs.

This result initially suggests that there could be other factors beyond the orientation of the obscuring torus that dictate the differences between broad-line SMGs and X-ray-obscured SMGs. Indeed, as can be seen in Figure 3, the X-ray luminosities for three of the broad-line SMGs are $\approx$10 times higher than the other broad-line SMGs and the X-ray-obscured SMGs. The average black-hole mass and Eddington ratio of these X-ray-luminous broad-line SMGs ($L_{\rm X} \approx 10^{45}$ erg s^{-1}) is

$\log(M_{\rm BH}/M_\odot) = 8.2$–$8.6$ and $\eta \approx 0.4$–0.9, with an overall average of $\log(M_{\rm BH}/M_\odot) \approx 8.4$ and $\eta \approx 0.6$. These black-hole masses and Eddington ratios are similar to the average found for SDSS quasars with FWHM < 3500 km s^{-1} ($\log(M_{\rm BH}/M_\odot) = 8.5$; $\eta \approx 1.0$); see Figure 2. The X-ray-luminous broad-line SMGs may therefore be more closely related to the submm-detected quasars studied by Page et al. (2001, 2004) and Stevens et al. (2005) and are potentially more evolved objects than the X-ray-obscured SMGs (e.g., Coppin et al. 2008).

In contrast, the average black-hole mass and Eddington ratio of the lower-luminosity broad-line SMGs ($L_{\rm X} \approx 10^{44}$ erg s^{-1}) is $\log(M_{\rm BH}/M_\odot) = 7.8$–$8.2$ and $\eta \approx 0.1$–0.3, depending upon the geometry of the BLR gas (see Section 3.2), with an overall average of $\log(M_{\rm BH}/M_\odot) \approx 8.0$ and $\eta \approx 0.2$. The X-ray-obscured SMGs lie in the same location of the $L_{\rm X}$–$L_{\rm FIR}$ plane as the lower-luminosity broad-line SMGs, providing evidence that they are intrinsically similar systems where the nucleus is obscured at optical wavelengths in the X-ray-obscured SMGs (e.g., Antonucci 1993). Under this scenario, the black-hole masses of the X-ray-obscured SMGs can be constrained from the Eddington ratios of the broad-line SMGs; see Equation (1). Since all of the lower-luminosity broad-line SMGs have $\eta > 0.1$, the estimated black-hole masses of the X-ray-obscured SMGs will be $\log(M_{\rm BH}/M_\odot) < 8.1$, and the average black-hole mass will be $\log(M_{\rm BH}/M_\odot) \approx 7.8$ for the average Eddington ratio of $\eta \approx 0.2$; we provide further evidence for $\eta = 0.2$ in Section 4.

3.5. The Black-Hole–Galaxy Mass Relationship for X-Ray-Obscured SMGs

We can combine the black-hole mass constraints with host-galaxy masses to extend the analyses of Borys et al. (2005) and explore the black-hole–galaxy mass relationship for the X-ray-obscured SMGs. The stellar-mass constraints from Borys et al. (2005) were calculated for the X-ray-obscured SMGs in Alexander et al. (2005a, 2005c) using rest-frame UV–near-IR observations (ground-based, *Hubble Space Telescope*, and *Spitzer* imaging). Adopting appropriate mass-to-light ratios for the stellar populations in these systems ($L_{\rm K}/M \approx 3.2$), Borys et al. (2005) found a mean stellar mass of $2.5 \times 10^{11}\ M_\odot$ for all of the SMGs. However, excess rest-frame UV or near-IR emission beyond that expected from starlight indicates that AGN activity is probably contaminating the stellar continuum in four galaxies (see Table 3 of Borys et al. 2005). Furthermore, the sample included three $z \lesssim 1$ galaxies, which have lower redshifts than the broad-line SMGs. Therefore, when calculating the average stellar masses here we have only considered the six $z > 1.8$ X-ray-obscured SMGs that do not have a UV or near-IR excess in Borys et al. (2005), giving a mean stellar mass of $2.2 \times 10^{11}\ M_\odot$, a factor $\approx$2 less than the mean of all of the $z > 1.8$ X-ray-obscured SMGs in Borys et al. (2005; $M_{\rm GAL} \approx 4.5 \times 10^{11}\ M_\odot$). This stellar mass estimate is consistent with the galactic masses estimated from the CO dynamics ($(1.2 \pm 1.5) \times 10^{11}\ M_\odot$; Greve et al. 2005; see Swinbank et al. 2004, 2006 for similar Hα dynamical constraints). The Maraston (2005) stellar population models, which take into account thermally pulsating asymptotic giant branch (TP-AGB) stars, would predict similar stellar masses if the starbursts in SMGs are long lived, as typically assumed. However, even in a less likely scenario where the starbursts in SMGs are short lived (i.e., $\lesssim$10 Myrs; which leads to improbably high space densities for the $z \approx 0$ descendants of SMGs), the stellar masses estimated from the Maraston (2005) model are still only $\lesssim$3 times lower than those given here (see A. M. Swinbank et al. 2008, in preparation, for a detailed discussion).

The local black-hole–galaxy mass relationship that we have adopted here is based on the galaxy spheroid rather than the entire galaxy. The CO dynamical constraints of Greve et al. (2005) trace the mass within the central $\approx$2kpc of SMGs, where the majority of the CO gas lies (e.g., Tacconi et al. 2006), while the stellar masses will include the whole galaxy. Since the effective radius for early-type galaxies with $M_{\rm GAL} > 10^{11}\ M_\odot$ is >4kpc (see Figure 2 of Desroches et al. 2007 for $M_{\rm R} \gtrsim -21.5$ ($\approx L_*$); Bell et al. 2003), the CO gas is tracing scales smaller than the spheroid and therefore provides a lower limit to the spheroid mass. We also note here that the CO dynamical constraint includes all baryonic material, not just the stars; however, the gas is likely to be ultimately converted to stars in these systems. Similarly, the stellar mass is $\approx$2 times the CO dynamical mass and corresponds to the entire galaxy. However, since the surface-brightness distributions of most SMGs are reasonably well fitted with a spheroid-like $r^{1/4}$ profile (C. Borys et al. 2008, in preparation), the stellar masses of these galaxies are likely to be dominated by the spheroid. Furthermore, we note that if SMGs are massive elliptical galaxies in formation (e.g., Blain et al. 2004; Swinbank et al. 2006; Tacconi et al. 2006), as commonly assumed, then any non-spheroid component in the host galaxy is likely to be subsumed within the existing spheroid component. In this scenario, the entire stellar mass would ultimately represent the final galaxy spheroid mass of the system.

In Figure 4, we plot the black-hole versus galaxy mass for the $z > 1.8$ X-ray obscured SMGs, with the objects with excess emission removed; the average estimated black-hole mass of these objects is the same as that given for the full sample in Section 3.4 ($\log(M_{\rm BH}/M_\odot) \approx 7.8$; i.e., $\log(M_{\rm BH,Edd}/M_\odot) \approx 7.1$). The average black-hole–galaxy mass ratio of the X-ray-obscured SMGs is $\approx 2.9 \times 10^{-4}$ and $\approx 5.3 \times 10^{-4}$ for the average stellar mass and CO dynamical mass, respectively. Assuming the black-hole–spheroid mass relationship of Häring & Rix (2004), the SMGs lie $\approx$3–5 times below that found for comparably massive normal galaxies in the local Universe, with considerable uncertainty, depending upon whether the average CO dynamical mass or stellar mass is used. If the Marconi & Hunt (2003) relationship adopted by Borys et al. (2005) is used then the SMGs would lie $\approx$1.4 times further below the local relationship. The average black-hole–galaxy mass ratio that we estimate for the X-ray-obscured SMGs is an order of magnitude higher than that estimated in Borys et al. (2005). The primary reason for this difference is due to using $\eta = 0.2$ (rather than $\eta = 1.0$ assumed by Borys et al. 2005), although the exclusion of the SMGs with excess emission also contributes to the higher value determined here.

4. COMPARISON TO NEARBY ULIRGs

Our analyses in Section 3 provided the first quantitative estimates of the black-hole masses and black-hole–galaxy mass relationship of the SMG population. We estimated the black-hole masses of the X-ray-obscured SMGs under the assumption that they are the obscured counterparts of the lower-luminosity broad-line SMGs, finding $\log(M_{\rm BH}/M_\odot) \approx 7.8$ for $\eta \approx 0.2$. However, there are a number of uncertainties that could be better constrained. First, it would be useful to have independent black-hole mass constraints for the X-ray-obscured SMGs, to reduce the need to make assumptions about their relationship with the broad-line AGNs and to minimize the potential inclination-

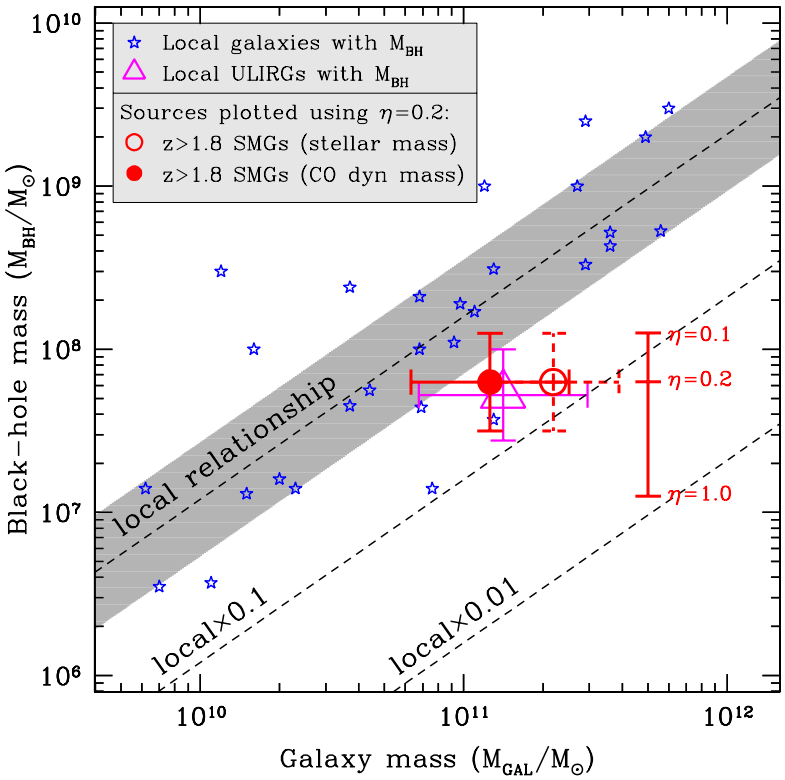

Figure 4. Black-hole versus galaxy mass. We plot the estimated average properties of the X-ray-obscured SMGs for different host-galaxy mass measurements (CO dynamics; Greve et al. 2005; stellar masses; Borys et al. 2005), assuming $\eta = 0.2$. We also plot the average properties of the obscured ULIRGs with broad Paα emission (see Section 4.1) and show the properties of well-studied nearby galaxies (taken from Häring & Rix 2004). The error bars correspond to 1σ uncertainties on the average properties. The shaded region indicates the black-hole–spheroid mass relationship from Häring & Rix (2004) and the dashed lines indicate different ratios of this relationship. The solid bar indicates the black-hole mass constraints for the X-ray-obscured SMGs for different Eddington ratios. For $\eta = 0.2$, the SMGs lie ≈3–5 times below this relationship, depending upon whether the average CO dynamical mass or stellar mass constraints are used; these results are qualitatively consistent with those found for the nearby obscured ULIRGs.

(A color version of this figure is available in the online journal)

dependent effects on the widths of the broad emission lines. Second, the determination of the black-hole masses of the X-ray-obscured SMGs depend upon accurate intrinsic X-ray luminosities, which relies on correcting the observed X-ray luminosities for the effect of absorption. We deal with these two issues here by studying nearby ULIRGs that host obscured AGNs. The advantage of this approach is that the observations of nearby ULIRGs are often more extensive and of a considerably higher signal-to-noise ratio than that obtained for distant SMGs, although clearly the disadvantage is that we will be studying objects at a different epoch to the SMGs. However, the similarity in the properties of SMGs and the nearby ULIRGs, and the fact that they both appear to be major-merger induced events suggests that SMGs could be "scaled-up" versions of ULIRGs (e.g., Tacconi et al. 2006), providing some support for our general approach (see Section 2.2).

4.1. Are the Eddington Ratios Smaller for the X-Ray Obscured SMGs?

Although the presence of obscuration prevents the opportunity to measure the black-hole properties of the X-ray obscured SMGs, the identification of broad Paα emission provides the chance to constrain $M_{\rm BH}$ and η in a small number of nearby ULIRGs hosting obscured AGNs (e.g., Veilleux et al. 1997, 1999). The broad-line emission from these sources is thought to be observed through the atmosphere of the dusty torus, which is assumed to be optically thin at near-IR wavelengths. A benefit of focusing on obscured AGNs is that any potential inclination-dependent effects on the black-hole mass and Eddington ratio will be minimized since the BLR is unlikely to be seen close to pole on.

Out of the sample of 64 nearby obscured ULIRGs observed by Veilleux et al. (1997, 1999), six have broad Paα emission; see Table 2 for their properties. We determined the black-hole masses of these objects using the Greene & Ho (2005) virial black-hole mass estimator by correcting the Paα luminosity to that expected for Hα using the Case B approximation (Hα/Paα = 8.6; e.g., Hummer & Storey 1987); see Figure 1. In Figure 2, we show the mass accretion rate versus virial black-hole mass for the four obscured ULIRGs that have sensitive X-ray constraints. The mass accretion rates were estimated from the absorption-corrected X-ray luminosity following Section 3.3, and we converted to the 0.5–8.0 keV band assuming $\Gamma = 1.8$, when necessary. The Eddington ratios of these obscured ULIRGs range from $\eta = 0.1$–0.5, with an average of $\eta = 0.2^{+0.2}_{-0.1}$. The average Eddington ratio is similar to that found for the lower-luminosity broad-line SMGs, further suggesting that $\eta \approx 0.2$ is a good choice for the X-ray-obscured SMGs.

4.2. Have the Intrinsic Luminosities of the X-Ray-Obscured SMGs been Underestimated?

The estimated black-hole masses of the X-ray-obscured SMGs are heavily dependent on how accurately the intrinsic

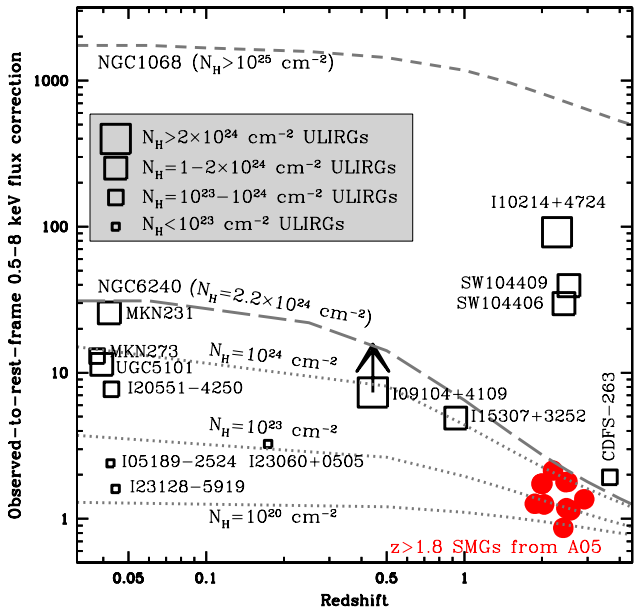

Figure 5. X-ray flux absorption corrections versus redshift for X-ray-obscured AGNs in ULIRGs at low and high redshifts (taken from Brandt et al. 1997; Franceschini et al. 2000, 2003; Severgnini et al. 2001; Imanishi et al. 2003; Ptak et al. 2003; Braito et al. 2004; Alexander et al. 2005b; Balestra et al. 2005; Mainieri et al. 2005; Polletta et al. 2006) and the $z > 1.8$ X-ray-obscured SMGs studied in Alexander et al. (2005a). The corrections that would need to be made for two nearby Compton-thick AGN NGC 1068 (dashed curve; using Matt et al. 1997 model) and NGC 6240 (long dashed curve; using Vignati et al. 1999 model) are shown in addition to the models adopted by Alexander et al. (2005a) for lower amounts of obscuration (dotted curves); the assumed column densities are indicated. The X-ray-derived column densities for the ULIRGs are indicated using different symbol sizes. The negative K-corrections for AGNs in the X-ray band mean that the absorption corrections are not large for high-redshift objects unless they are heavily Compton thick (i.e., $N_H \gg 10^{24}$ cm^{-2}). The good agreement between the absorption corrections used in Alexander et al. (2005a) and those of obscured ULIRGs in the literature indicate that the intrinsic X-ray luminosities of the X-ray-obscured SMGs are unlikely to be significantly underestimated.

(A color version of this figure is available in the online journal)

luminosity of the AGN (and hence the Eddington-limited black-hole mass; Alexander et al. 2005c) is calculated. The X-ray spectra produced for the X-ray-obscured SMGs in Alexander et al. (2005a) showed that the majority of the AGNs are heavily obscured (≈80% have $N_H > 10^{23}$ cm^{-2}), indicating that potentially large absorption corrections may need to be applied to calculate the intrinsic X-ray luminosities. Given the poor photon statistics for the X-ray spectra of individual objects, it is useful to verify that the adopted absorption corrections used in Alexander et al. (2005a) are typical for obscured AGNs. This is particularly important for the most heavily obscured AGNs as the corrections become increasingly model dependent as the absorption approaches and exceeds Compton-thick obscuration (i.e., $N_H = 1.5 \times 10^{24}$ cm^{-2}) due to uncertain contributions from reflected and scattered AGN components (e.g., Mushotzky et al. 1993; Matt et al. 2000).

In Figure 5, we show the applied absorption corrections for the $z > 1.8$ X-ray obscured SMGs in Alexander et al. (2005a) and compare them to those adopted in other X-ray spectral analysis studies of low- and high-redshift ULIRGs. The absorption corrections applied to the SMGs are in good agreement with those used in other studies, indicating that unless the X-ray-obscured SMGs are more heavily obscured than estimated in Alexander et al. (2005a), their intrinsic X-ray luminosities are not significantly underestimated (i.e., $L_X \approx 10^{44}$ erg s^{-1}). Faint *Spitzer*–IRS spectroscopy also shows that the AGN activity in SMGs is typically weak at mid-IR wavelengths, in good agreement with that implied by their X-ray luminosities, assuming typical X-ray–mid-IR conversions for AGNs (e.g., Menéndez-Delmestre et al. 2007; Valiante et al. 2007; Pope et al. 2008).

The poor photon statistics for the individual X-ray spectra of the X-ray-obscured SMGs in Alexander et al. (2005a) can also lead to significant uncertainties on the measured absorption. In an attempt to minimize this, Alexander et al. (2005c) constructed composite rest-frame 2–20 keV spectra for the SMGs grouped into three different absorption bands: $N_H < 10^{23}$ cm^{-2}, $N_H = (1–5) \times 10^{23}$ cm^{-2}, and $N_H > 5 \times 10^{23}$ cm^{-2}. These composite X-ray spectra validated the individual X-ray spectral analyses and showed that the average intrinsic X-ray luminosity of the most heavily obscured AGNs is comparable to that of the less obscured AGNs (where the absorption corrections are smaller), as expected if all sources have the same intrinsic AGN properties but some are more heavily obscured (e.g., Antonucci 1993; Mushotzky et al. 1993; Smith & Done 1996). However, the composite X-ray spectra still only had moderately good photon statistics (≈600–1000 X-ray counts; see Figure 7 of Alexander et al. 2005a), and validation of the estimated column densities would be useful. Better statistics could be achieved by the identification of more SMGs hosting AGN activity in the *Chandra* Deep Fields, which should be possible with the advent of the ultra-deep 450 μm/850 μm SCUBA2 Cosmology Legacy Surveys, or from deeper X-ray exposures in these fields.[12] However, in the immediate absence of these two possibilities, a reasonable alternative is to compare the properties of the AGNs in the X-ray-obscured SMGs to the AGNs in nearby ULIRGs, where the signal-to-noise ratio of the data is higher.

The initial ULIRG sample selected for this analysis comprises the ten ULIRGs at $d < 200$ Mpc from the *IRAS* Revised Bright Galaxy Sample (RBGS; Sanders et al. 2003). By restricting our comparison to the closest ULIRGs, we ensure homogenous, high signal-to-noise hard X-ray data (all of the galaxies have *Chandra* data and nine galaxies have *XMM-Newton* data); the X-ray coverage of ULIRGs at $d > 200$ Mpc is considerably poorer. Due to the larger effective area of *XMM-Newton* over *Chandra* at >6 keV, where the Fe Kα emission line and photo-electric cutoff for heavily obscured nearby AGN are present, the X-ray properties of the AGNs used in these analyses are only taken from *XMM-Newton* observations (Severgnini et al. 2001; Franceschini et al. 2003; Imanishi et al. 2003; Braito et al. 2004; Balestra et al. 2005).

Six (60^{+35}_{-24}%; errors calculated from Gehrels 1986) of the 10 $d < 200$ Mpc ULIRGs show evidence for AGN activity at X-ray energies and all are heavily obscured ($N_H > 10^{22}$ cm^{-2}); see Table 3 for the properties of these objects. In Figure 6, we show the absorption-corrected X-ray–far-IR luminosity ratio versus the X-ray measured absorption column density of these sources and compare them to the $z > 1.8$ X-ray-obscured SMGs from Alexander et al. (2005a). Although selection effects may be present, the AGN properties of these two populations are similar (average $\log(N_H) \approx 23.8$ cm^{-2} and $\log(L_X/L_{FIR}) \approx -2.5$), indicating that the properties of the AGNs in the SMGs are comparable to those found in the

[12] See http://www.jach.hawaii.edu/JCMT/surveys/Cosmology.html for details of the SCUBA2 Cosmology Legacy Surveys.

Table 2
Obscured ULIRGs with Broad Paα Emission

Name	d_L (Mpc)	$\log(L_{Pa\alpha})^a$ (erg s^{-1})	FWHM$_{Pa\alpha}$ (km s^{-1})	$\log(M_{BH})$ ($M_\odot$)	$\log(L_X)^{a,b}$ (erg s^{-1})	$M_K{}^a$ (mag)	Refs
I05189−2524	169	41.8	2600	7.4	43.3	−24.7	1, 2, 3
I13305−1739	695	41.9	2900	7.6	...	−26.0	1, 3
PKS1345+12	563	42.3	2600	7.7	43.4	−26.1	3, 4, 5
I20460+1925	868	43.1	2900	8.2	44.2	...	4, 6
I23060+0505	831	42.9	2000	7.8	44.3	−25.5	3, 4, 7
I23498+2423	1036	43.0	3000	8.2	...	−26.9	3, 4

Notes.
[a] Recalculated from the published value using the given luminosity distance.
[b] Rest-frame 2–10 keV band, corrected for absorption.
References.
(1) Veilleux et al. (1999); (2) Severgnini et al. (2001); (3) Veilleux et al. (2002); (4) Veilleux et al. (1997); (5) O'Dea et al. (2000); (6) Ogasaka et al. (1997); (7) Brandt et al. (1997).

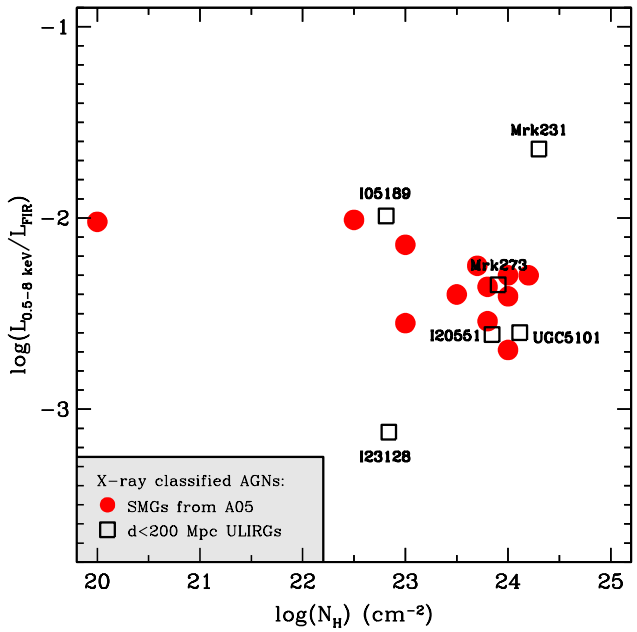

Figure 6. Unabsorbed 0.5–8.0 keV-to-far-IR luminosity ratio versus X-ray-derived column densities for the $z > 1.8$ X-ray-obscured SMGs from Alexander et al. (2005a) and the six $d < 200$ Mpc ULIRGs hosting obscured AGN activity (see Section 4.2). The far-IR luminosities for the X-ray-obscured SMGs are from Alexander et al. (2005a) and are calculated using the radio-to-far-IR relationship, and the far-IR luminosities for the $d < 200$ Mpc ULIRGs are taken from Sanders et al. (2003). The column density and X-ray-to-far-IR luminosity ratio distributions of both populations are similar.
(A color version of this figure is available in the online journal)

nearby ULIRGs, despite being significantly more distant and luminous.

Lastly, we briefly consider the possibility that a significant fraction of the AGN luminosity is undetected in the <10 keV observed-frame data (e.g., due to the presence of extreme Compton-thick absorption; $N_H > 10^{25}$ cm^{-2}). Current ultra-hard (≈10–100 keV) X-ray observatories are not sensitive enough to place stringent constraints on the >10keV emission from X-ray-obscured SMGs. However, we note that the six X-ray-detected AGNs in the $d < 200$ Mpc ULIRG sample have >10 keV constraints from *BeppoSAX*-PDS and the *Swift*-BAT survey (e.g., Severgnini et al. 2001; Braito et al. 2004; Markwardt et al. 2005; Dadina 2007) which already rule out the presence of an AGN component >5 times more luminous than

Table 3
$d < 200$ Mpc ULIRGs Hosting AGN Activity

Name	$d_L{}^a$ (Mpc)	$\log(L_{FIR})^a$ ($L_\odot$)	$\log(L_X)^{b,c}$ (erg s^{-1})	$\log(N_H)$ (cm^{-2})	Refs
I05189−2524	169	12.0	43.5	22.8	1
UGC 5101	159	11.9	42.8	24.1	2
MKN 231	172	12.3	44.2	24.3	3
MKN 273	155	12.1	43.0	23.8	4
I20551−4250	173	11.9	43.1	23.9	5
I23128−5919	178	12.0	42.4	22.8	5

Notes.
[a] Taken from Sanders et al. (2003).
[b] Recalculated from the published value using the given luminosity distance.
[c] Rest-frame 2–10 keV band, corrected for absorption.
References.
(1) Severgnini et al. (2001); (2) Imanishi et al. (2003); (3) Braito et al. (2004); (4) Balestra et al. (2005); (5) Franceschini et al. (2003).

that estimated from the *XMM-Newton* data for these sources; see Figure 3.

The similarity in the column densities and X-ray-to-far-IR luminosity ratios of the $d < 200$ Mpc ULIRGs and the X-ray-obscured SMGs suggest that the intrinsic X-ray luminosities of the SMGs are unlikely to be significantly higher than those estimated in Alexander et al. (2005a). We therefore conclude that the average X-ray-derived black-hole masses of the X-ray-obscured SMGs are unlikely to be significantly higher (i.e., by factors $\gtrsim$2) than the constraints given in Section 3.

4.3. The Black-Hole–Galaxy Mass Relationship for Nearby Obscured ULIRGs

With black-hole masses for the obscured ULIRGs, we can take the same approach as for the SMGs and determine the black-hole–galaxy mass relationship for these galaxies. In Figure 4, we show the black-hole versus galaxy mass for the obscured ULIRGs with broad Paα emission; the statistics are too poor for the $d < 200$ Mpc ULIRG sample since only three objects have stellar mass constraints and only one object has a black-hole mass constraint. The galaxy masses were calculated using AGN-subtracted K-band host-galaxy magnitudes from Veilleux et al. (2002), adopting the same mass-to-light ratio as that used by Borys et al. (2005; $L_K/M = 3.2$) for the SMGs; see Table 2. The average black-hole-to-galaxy mass ratio of the obscured ULIRG sample is consistent with those of the SMGs. This is significant since both the black-hole and galaxy mass constraints were determined directly for these ULIRGs,

reducing the number of potential uncertainties in the derived $M_{\rm BH}$–$M_{\rm GAL}$ ratio. As for the SMGs, the stellar masses of the ULIRGs are for the entire galaxy; however, since ≈73% of ULIRGs have an elliptical-like $r^{1/4}$ surface-brightness profiles (Veilleux et al. 2002), the stellar mass will be dominated by the galaxy spheroid. Furthermore, the luminosity, R-band axial ratio, velocity dispersion distribution, and location of nearby ULIRGs on the fundamental place already closely resemble those of intermediate-mass elliptical galaxies (e.g., Genzel et al. 2001; Veilleux et al. 2002; Dasyra et al. 2006), suggesting that the stellar mass is tracing the ultimate mass of the system.

We therefore conclude that we see qualitatively similar behavior in both the SMGs and the nearby ULIRGs. Since the nearby ULIRGs are easier to study in detail than the more distant SMGs, they could potentially provide future insight into the evolutionary status of these galaxy populations (e.g., Hao et al. 2005; Kawakatu et al. 2006).

5. DISCUSSION

The primary aim of this paper has been to provide quantitative constraints on the black-hole masses and evolutionary status of the SMG population. Using virial black-hole mass estimates, we constrain the black-hole masses of $z > 1.8$ X-ray obscured SMGs to be $\log(M_{\rm BH}/M_\odot) \approx 7.8$ for $\eta = 0.2$. When combined with host-galaxy mass constraints, the black holes of the X-ray-obscured SMGs appear to be ≈3–5 times smaller than those found for comparably massive galaxies in the local Universe, implying that the growth of the black hole lags that of the host galaxy in SMGs. We provided corroborating evidence for this result from analyses of nearby obscured ULIRGs, potentially the $z \approx 0$ analogs of the X-ray obscured SMGs. In this final section we compare our results to those found for $z \approx 2$ radio galaxies and quasars and explore the evolutionary status and black-hole growth of the X-ray-obscured SMGs.

5.1. Comparison to $z \approx 2$ Optically Luminous Quasars and Radio Galaxies

Our results for the X-ray-obscured SMGs are statistically inconsistent with investigations of $z \approx 2$ radio galaxies and luminous quasars, where it has been found that the black holes hosted by these objects are up to ≈6 times larger than those found for comparably massive galaxies in the local universe (e.g., McLure et al. 2006; Peng et al. 2006). We demonstrate this in Figure 7, where we show the black-hole–galaxy mass ratio versus redshift for the X-ray-obscured SMGs and compare them to the $z \approx 2$ radio galaxies and quasars and the $z \approx 0$ obscured ULIRGs with black-hole mass constraints. To be consistent with the results of Peng et al. (2006), the black holes in the SMGs would need to be $\gtrsim$10 times more massive than those estimated here (i.e., $M_{\rm BH} \gtrsim 10^9\ M_\odot$). However, none of the broad-line SMGs in our sample have such high black-hole masses, even allowing for potential BLR inclination angle effects. Furthermore, black holes with $M_{\rm BH} \gtrsim 10^9\ M_\odot$ are rare even in the local universe, with a space density of $\phi \approx 10^{-5}$ Mpc^{-3} (e.g., McLure & Dunlop 2004), which is comparable to the observed space density of $z \approx 2$ SMGs and about an order of magnitude lower than the SMG space density *corrected* for a 300 Myr submm-bright phase ($\phi \approx 1.3 \times 10^{-4}$ Mpc^{-3}; see Section 4.2 of Swinbank et al. 2006). These analyses show that the $z \approx 0$ descendants of typical SMGs cannot host massive black holes of $M_{\rm BH} \gtrsim 10^9\ M_\odot$ and therefore suggest that the most luminous radio galaxies and quasars investigated by

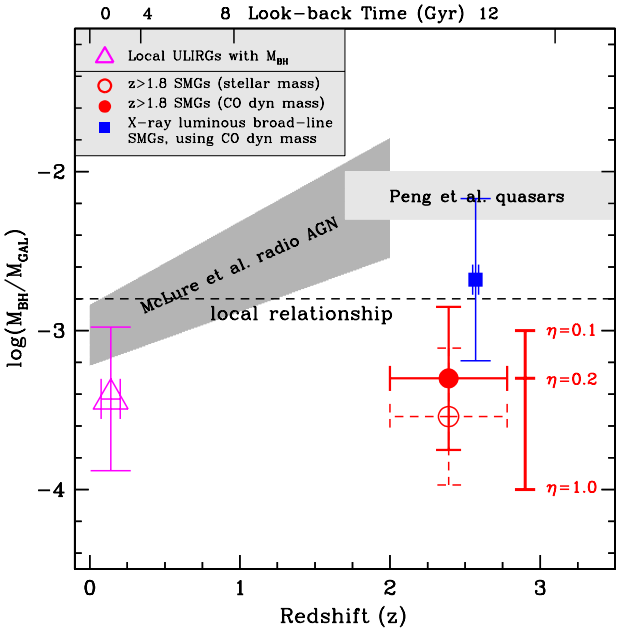

Figure 7. Black-hole–host-galaxy mass ratio versus redshift for the $z > 1.8$ X-ray-obscured SMGs, X-ray-luminous broad-line SMGs, and the obscured ULIRGs with broad Paα emission. The $z > 1.8$ X-ray-obscured SMGs are plotted using the stellar mass and the CO dynamical mass constraints. The dashed line indicates the local black-hole–spheroid mass relationship from Häring & Rix (2004), the dark-shaded region shows the radio galaxy constraints from McLure et al. (2006), and the light-shaded region indicates the constraints for $z \approx 2$ quasars from Peng et al. (2006). The error bars correspond to 1σ uncertainties. The X-ray-obscured SMGs lie marginally below the local relationship (factor ≈3–5), as also found for the nearby obscured ULIRGs, and they lie a factor $\gtrsim$10 below that found for $z \approx 2$ radio galaxies and quasar population. This suggests that SMGs are identified at an earlier stage in the evolution of quasars and massive galaxies. The X-ray-luminous broad-line SMGs are statistically consistent with the local relationship, assuming the CO dynamical mass constraints from the SMGs and the average Eddington ratio of $\eta = 0.6$. We discuss the overall constraints in Section 5.

(A color version of this figure is available in the online journal)

McLure et al. (2006) and Peng et al. (2006) have a different evolutionary path to the SMGs. Indeed, given the significantly larger fraction of radio galaxies that are submm-detected at $z > 2.5$ when compared to the submm-detected fraction of radio galaxies at $z < 2.5$ ($\gtrsim$75% at $z > 2.5$ versus ≈15% at $z < 2.5$; Archibald et al. 2001), it seems likely that these galaxies (which represent the most massive galaxies at every epoch; Seymour et al. 2007) underwent their major star-formation phases at higher redshifts than the SMG population. We note that this conclusion is also consistent with detailed spectral fitting of the stellar populations of nearby massive galaxies (e.g., Nelan et al. 2005; Panter et al. 2007).

However, it is also possible that the variations in the $M_{\rm BH}$–$M_{\rm GAL}$ relationship at $z \approx 2$ are due to selection effects, as first suggested by Lauer et al. (2007). The selection of the most luminous quasars and radio galaxies will clearly identify the most massive black holes since the Eddington limit restricts the luminosity of small accreting black holes, potentially causing a bias toward objects with large $M_{\rm BH}$–$M_{\rm GAL}$ ratios. It is not clear that the selection of SMGs will cause an opposite bias since there is not an equivalent stellar-mass-based Eddington-limited restriction in star-forming galaxies. However, empirically, the galaxies that are undergoing the most intense star formation at $z \approx 2$ also appear to be massive galaxies at this epoch (e.g., Papovich et al. 2006), suggesting that the selection of SMGs

will cause a bias toward the identification of massive galaxies. However, this selection is probably not as closely coupled to a bias in the $M_{\rm BH}$–$M_{\rm GAL}$ as the selection of radio galaxies and quasars.

5.2. The Evolutionary Status and Black-Hole Growth of SMGs

Our results show that the $z \approx 0$ descendants of SMGs cannot host black holes with $M_{\rm BH} \gtrsim 10^9\ M_\odot$. Indeed, on the basis of dynamical mass estimates, stellar luminosities, and star-formation lifetimes, Swinbank et al. (2006) have shown that the local descendants of SMGs are likely to be $\gtrsim 3L_*$ early-type galaxies ($M_{\rm GAL} \gtrsim 3 \times 10^{11}\ M_\odot$, assuming the Bell et al. (2003) luminosity and stellar-mass functions), with space densities of $\approx 10^{-4}$ Mpc^{-3}. We therefore expect the $z \approx 0$ descendants of SMGs to host black holes with $M_{\rm BH} \gtrsim 4 \times 10^8\ M_\odot$, comparable to those of the X-ray-luminous broad-line SMGs. This would suggest that the black holes of SMGs and their descendants typically only need to grow by a factor of $\approx$6 by the present day. Can we account for this black-hole growth in the estimated submm-bright lifetime of SMGs ($\approx$100–300 Myr)?

Assuming that the black holes in the X-ray-obscured SMGs are growing at $\eta \approx 0.2$ (the average Eddington rate estimated in Section 3.4), it will take $\approx$400 Myr for them to increase in mass by a factor $\approx$6. Since we are likely to be observing a typical SMG halfway through its submm-bright phase, this lifetime is longer than the remaining gas consumption timescale (i.e., $\approx$150 Myr, taking the $\approx$300 Myr total lifetime estimated by Swinbank et al. 2006). However, as mentioned in Section 3.4, the Eddington ratios derived for the broad-line SMGs should only be considered indicative and it is possible that the X-ray-obscured SMGs are growing their black holes at $\eta > 0.2$. For example, taking the latest derivation of bolometric corrections from Vasudevan & Fabian (2007) for high accretion rate AGNs, the estimated Eddington ratio would be $\eta \approx 0.4$ (i.e., $\kappa_{2-10\,\rm keV} \approx 70$; see Section 3.3), which is sufficient for a black hole to grow by a factor $\approx$6 in $\approx$200 Myr and broadly consistent with current estimates for the submm-bright lifetime of SMGs.

We can also take the alternative approach adopted by Kawakatu et al. (2007b) for local ULIRGs, and assume that the bolometric luminosity produced by SMGs is entirely due to AGN activity. Under this hypothesis, we would estimate Eddington ratios of $\eta \approx 2$ (i.e., for a mean $L_{\rm FIR} \approx 5 \times 10^{12}\ M_\odot$; see Figure 3). However, we consider this scenario too extreme since all of the current evidence indicates that star-formation dominates the bolometric luminosity of typical SMGs, as witnessed by (1) the correlation between far-IR luminosity and reddening corrected Hα star-formation rate (SFR) (e.g., Swinbank et al. 2004; Takata et al. 2006), (2) the strong polycyclic aromatic hydrocarbon (PAH) features seen in their mid-IR spectra and the correlation between the luminosity of the PAH emission and the total IR luminosity (e.g., Menéndez-Delmestre et al. 2007; Pope et al. 2008), (3) the extended radio emission in high-resolution (<4 kpc) maps (e.g., Chapman et al. 2004; Biggs & Ivison 2008), and (4) the absorption-corrected X-ray-to-far-IR luminosities, which indicate that AGN activity contributes $\approx$10% of the bolometric luminosity (e.g., Alexander et al. 2005a). All of these facts suggest that the bolometric luminosity of SMGs is dominated by star formation, and therefore this determination of the Eddington ratio provides a firm upper limit.

Finally, we consider the properties of the X-ray-luminous ($L_{\rm X} \approx 10^{45}$ erg s^{-1}) broad-line SMGs; see Section 3.4. These objects have more massive black holes than the X-ray obscured SMGs and they might represent transition objects between typical SMGs and typical unobscured quasars (e.g., Coppin et al. 2008); see Figure 7 for constraints on their $M_{\rm BH}$–$M_{\rm GAL}$ ratio, assuming that they have host-galaxy masses comparable to the X-ray-obscured SMGs. The location of the X-ray-luminous broad-line SMGs in the $L_{\rm X}$–$L_{\rm FIR}$ plane indicates that these objects might be similar to the submm-detected quasars identified by Page et al. (2001, 2004) and Stevens et al. (2005). It has been argued that submm-detected quasars represent a late stage in the evolution of SMGs (e.g., Coppin et al. 2008), where accretion-related outflows from the black hole have started to remove gas and dust from the nucleus and the host galaxy (as suggested by most models; e.g., Sanders et al. 1988; Di Matteo et al. 2005; King 2005; Granato et al. 2006; Hopkins et al. 2006a; Chakrabarti et al. 2008). A natural consequence of these accretion-related outflows should be a decrease in the fraction of luminous obscured AGNs. It is therefore interesting that current submm surveys have not yet identified a large population of luminous X-ray-obscured quasars (see Bautz et al. 2000; Mainieri et al. 2005; and Pope et al. 2008 for some objects), indicating that they are rare. The combination of the wide-area SCUBA2 Cosmology Legacy Survey (see Footnote 4) with moderately deep X-ray and IR coverage will provide the most definitive constraints on the ubiquity of submm-detected X-ray-obscured quasars and test whether they are transition objects between typical SMGs and typical unobscured quasars.

6. CONCLUSIONS

We have placed direct observational constraints on the black-hole masses ($M_{\rm BH}$) and Eddington ratios ($\eta = L_{\rm bol}/L_{\rm Edd}$) of the cosmologically important $z \approx 2$ SMG population, and used measured host-galaxy masses to explore their evolutionary status. Our main findings are the following.

1. We used the virial black-hole mass estimator to "weigh" the black holes in six SMGs with broad Hα or Hβ emission and found that they typically host black holes with $\log(M_{\rm BH}/M_\odot) \approx 8.0$–$8.4$ and $\eta \approx 0.2$–0.5, depending on the geometry of the broad-line region gas. These black holes are $\approx$0.4 dex smaller than those found for $z \approx 2$ optically bright quasars in the SDSS with comparably "narrow" broad lines. See Sections 3.1–3.3.
2. We found that the lower-luminosity broad-line SMGs ($L_{\rm X} \approx 10^{44}$ erg s^{-1}) lie in the same location of the $L_{\rm X}$–$L_{\rm FIR}$ plane as more typical SMGs hosting X-ray-obscured AGNs (X-ray-obscured SMGs). These two subsets of the SMG population may be intrinsically similar, where the rest-frame optical nucleus is visible in the broad-line SMGs (as suggested by the unified AGN model). Under this hypothesis, the X-ray-obscured SMGs host black holes of $\log(M_{\rm BH}/M_\odot) \approx 7.8$ with $\eta = 0.2$; we find corroborating evidence for $\eta \approx 0.2$ from detailed analyses of nearby obscured ULIRGs with broad Paα emission, potentially the local analogs of the X-ray-obscured SMGs. By comparison, the black holes and Eddington ratios of the X-ray-luminous broad-line SMGs ($L_{\rm X} \approx 10^{45}$ erg s^{-1}) are $\log(M_{\rm BH}/M_\odot) \approx 8.4$ and $\eta \approx 0.6$, suggesting that they are more evolved objects than typical SMGs. See Sections 3.4, 3.5, and 4.1.
3. We demonstrated that the X-ray-absorption corrections and estimated absorbing column densities of the X-ray-obscured SMGs are consistent with those typically found for nearby ULIRGs. This suggests that we have not significantly underestimated the intrinsic X-ray luminosities (and therefore the black-hole masses) of the X-ray-obscured SMGs. See Section 4.2.

4. We combined the black-hole mass constraints with measured host-galaxy masses ($M_{\rm GAL} \approx (1–2) \times 10^{11}\ M_{\odot}$). We found that X-ray-obscured SMGs typically host black holes $\gtrsim$3 times smaller than those found in comparably massive normal galaxies in the local universe, albeit with considerable uncertainty, and $\gtrsim$10 times smaller than those predicted for $z \approx 2$ populations. These results imply that the growth of the black hole lags that of the host galaxy in SMGs, in stark contrast with that previously found for optical and radio selected luminous quasars at $z \approx 2$, which is probably due to the SMGs being selected at an earlier evolutionary stage than the quasars. We also found that the growth of the black hole lags that of the host galaxy in local ULIRGs. See Sections 3.5, 4.3, and 5.
5. We provided evidence that the black holes of the descendants of SMGs are likely to be $M_{\rm BH} \approx 4 \times 10^8\ M_{\odot}$, rather than the $M_{\rm BH} \gtrsim 10^9\ M_{\odot}$ that would be required if they were to lie on the $M_{\rm BH}$–$M_{\rm GAL}$ relationship found for $z \approx 2$ radio galaxies and quasars. This implies that SMGs only need to grow their black holes by a factor ≈6 by the present day, which can be achieved within current estimates for the submm-bright lifetime of SMGs, provided that the black holes are growing at rates close to the Eddington limit. See Section 5.

The up-coming wide and deep SCUBA2 Cosmology Legacy Surveys will provide larger samples of SMGs with which to test these results and provide further insight into the relationship between the growth of massive black holes and their host galaxies in this cosmologically important $z \approx 2$ population. Significantly improved astrophysical insight into the AGN and host-galaxy properties of SMGs will be provided with the next generation of observatories over the coming decades. For example, mid-IR spectroscopy with the *James Webb Space Telescope* (*JWST*; Gardner et al. 2006) will yield constraints on the presence of broad emission lines in the rest-frame near-IR band, potentially providing a direct route to estimating the black-hole masses of the X-ray-obscured SMGs, and the Atacama Large Millimeter Array (ALMA; Kawakatu et al. 2007a; Wootten 2006) will provide resolved dynamical measurements of the host galaxy down to ≈100 pc scales, including the circumnuclear region around the black hole. If sufficiently sensitive optical and near-IR spectropolarimeters can be developed on 30–50 m telescopes, then it may also be possible to directly search for the presence of broad emission lines in scattered light in the X-ray-obscured SMGs (e.g., Antonucci & Miller 1985; Young et al. 1996). Finally, X-ray observations from planned and proposed telescopes over the next ≈10–15 years will provide the potential to constrain the energetics of the AGN activity, from either high signal-to-noise high-resolution spectroscopy or photometric measurements out to X-ray energies of ≈100 keV (e.g., the Japanese X-ray observatory *NEXT*, Ozawa et al. 2006; the NASA observatories *Constellation-X*, White et al. 2004 and *NuSTAR*, Harrison et al. 2005; and the ESA observatory *XEUS*, Parmar et al. 2006).

We gratefully acknowledge support from the Royal Society (DMA; IRS), STFC (AMS; KC), NASA LTSA grant NAG5-13035 (WNB), the *Chandra* Fellowship program (FEB), and the Alfred P. Sloan Foundation and Research Corporation (AWB). We thank M. Volonteri for insightful conversations, C. Maraston for discussing stellar-mass constraints based on her stellar evolution models, R. McLure for providing SDSS quasar data and useful feedback, and the anonymous referee for a thoughtful report.

REFERENCES

Adams, T. F., & Weedman, D. W. 1975, ApJ, 199, 19
Adelberger, K. L., & Steidel, C. C. 2005, ApJ, 627, L1
Alexander, D. M., Bauer, F. E., Chapman, S. C., Smail, I., Blain, A. W., Brandt, W. N., & Ivison, R. J. 2005a, ApJ, 632, 736
Alexander, D. M., Chartas, G., Bauer, F. E., Brandt, W. N., Simpson, C., & Vignali, C. 2005b, MNRAS, 357, L16
Alexander, D. M., Smail, I., Bauer, F. E., Chapman, S. C., Blain, A. W., Brandt, W. N., & Ivison, R. J. 2005c, Nature, 434, 738
Alexander, D. M., et al. 2003a, AJ, 126, 539
Alexander, D. M., et al. 2003b, AJ, 125, 383
Archibald, E. N., et al. 2001, MNRAS, 323, 417
Archibald, E. N., et al. 2002, MNRAS, 336, 353
Arshakian, T. G. 2005, A&A, 436, 817
Antonucci, R. 1993, ARA&A, 31, 473
Antonucci, R. R. J., & Miller, J. S. 1985, ApJ, 297, 621
Balestra, I., Boller, T., Gallo, L., Lutz, D., & Hess, S. 2005, A&A, 442, 469
Barger, A. J., Cowie, L. L., Sanders, D. B., Fulton, E., Taniguchi, Y., Sato, Y., Kawara, K., & Okuda, H. 1998, Nature, 394, 248
Bautz, M. W., Malm, M. R., Baganoff, F. K., Ricker, G. R., Canizares, C. R., Brandt, W. N., Hornschemeier, A. E., & Garmire, G. P. 2000, ApJ, 543, L119
Bell, E. F., McIntosh, D. H., Katz, N., & Weinberg, M. D. 2003, ApJS, 149, 289
Biggs, A. D., & Ivison, R. J. 2008, MNRAS, 385, 893
Blain, A. W., Chapman, S. C., Smail, I., & Ivison, R. 2004, ApJ, 611, 725
Borys, C., Chapman, S., Halpern, M., & Scott, D. 2003, MNRAS, 344, 385
Borys, C., Smail, I., Chapman, S. C., Blain, A. W., Alexander, D. M., & Ivison, R. J. 2005, ApJ, 635, 853
Bower, R. G., Benson, A. J., Malbon, R., Helly, J. C., Frenk, C. S., Baugh, C. M., Cole, S., & Lacey, C. G. 2006, MNRAS, 370, 645
Braito, V., et al. 2004, A&A, 420, 79
Brandt, W. N., Fabian, A. C., Takahashi, K., Fujimoto, R., Yamashita, A., Inoue, H., & Ogasaka, Y. 1997, MNRAS, 290, 617
Calzetti, D., Armus, L., Bohlin, R. C., Kinney, A. L., Koornneef, J., & Storchi-Bergmann, T. 2000, ApJ, 533, 682
Carilli, C. L., & Wang, R. 2006, AJ, 131, 2763
Chakrabarti, S., Fenner, Y., Hernquist, L., Cox, T. J., & Hopkins, P. F. 2008, ApJ, submitted (arXiv astro-ph/0610860)
Chapman, S. C., Blain, A. W., Smail, I., & Ivison, R. J. 2005, ApJ, 622, 772
Chapman, S. C., Smail, I., Windhorst, R., Muxlow, T., & Ivison, R. J. 2004, ApJ, 611, 732
Chapman, S. C., Windhorst, R., Odewahn, S., Yan, H., & Conselice, C. 2003, ApJ, 599, 92
Conselice, C. J., Chapman, S. C., & Windhorst, R. A. 2003, ApJ, 596, L5
Collin, S., Kawaguchi, T., Peterson, B. M., & Vestergaard, M. 2006, A&A, 456, 75
Coppin, K., et al. 2006, MNRAS, 372, 1621
Coppin, K., et al. 2008, MNRAS, submitted
Croton, D. J. 2006, MNRAS, 369, 1808
Dadina, M. 2007, A&A, 461, 1209
Dasyra, K. M., et al. 2006, ApJ, 651, 835
Desroches, L.-B., Quataert, E., Ma, C.-P., & West, A. A. 2007, MNRAS, 377, 402
Di Matteo, T., Springel, V., & Hernquist, L. 2005, Nature, 433, 604
Downes, D., & Eckart, A. 2007, A&A, 468, L57
Elvis, M., et al. 1994, ApJS, 95, 1
Fabian, A. C. 1999, MNRAS, 308, L39
Ferrarese, L., & Merritt, D. 2000, ApJ, 539, L9
Franceschini, A., Bassani, L., Cappi, M., Granato, G. L., Malaguti, G., Palazzi, E., & Persic, M. 2000, A&A, 353, 910
Franceschini, A., et al. 2003, MNRAS, 343, 1181
Gardner, J. P., et al. 2006, Space Sci. Rev., 123, 485
Gebhardt, K., et al. 2000, ApJ, 539, L13
Gebhardt, K., et al. 2003, ApJ, 583, 92
Gehrels, N. 1986, ApJ, 303, 336
Genzel, R., Tacconi, L. J., Rigopoulou, D., Lutz, D., & Tecza, M. 2001, ApJ, 563, 527
Granato, G. L., Silva, L., Lapi, A., Shankar, F., De Zotti, G., & Danese, L. 2006, MNRAS, 368, L72
Greene, J. E., & Ho, L. C. 2005, ApJ, 630, 122
Greve, T. R., Hainline, L. J., Blain, A. W., Smail, I., Ivison, R. J., & Papadopoulos, P. P. 2006, AJ, 132, 1938
Greve, T. R., et al. 2005, MNRAS, 359, 1165
Haas, M., Klaas, U., Müller, S. A. H., Chini, R., & Coulson, I. 2001, A&A, 367, L9

Hainline, L. J., Blain, A. W., Greve, T. R., Chapman, S. C., Smail, I., & Ivison, R. J. 2006, ApJ, 650, 614
Hao, C. N., Xia, X. Y., Mao, S., Wu, H., & Deng, Z. G. 2005, ApJ, 625, 78
Häring, N., & Rix, H.-W. 2004, ApJ, 604, L89
Harrison, F. A., et al. 2005, Exp. Astron., 20, 131
Heckman, T. M., Miley, G. K., van Breugel, W. J. M., & Butcher, H. R. 1981, ApJ, 247, 403
Hopkins, P. F., Hernquist, L., Cox, T. J., Di Matteo, T., Robertson, B., & Springel, V. 2006a, ApJS, 163, 1
Hopkins, P. F., Robertson, B., Krause, E., Hernquist, L., & Cox, T. J. 2006b, ApJ, 652, 107
Hughes, D. H., et al. 1998, Nature, 394, 241
Hummer, D. G., & Storey, P. J. 1987, MNRAS, 224, 801
Imanishi, M., & Terashima, Y. 2004, AJ, 127, 758
Imanishi, M., Terashima, Y., Anabuki, N., & Nakagawa, T. 2003, ApJ, 596, L167
Ivison, R. J., et al. 2002, MNRAS, 337, 1
Ivison, R. J., et al. 2004, ApJS, 154, 124
Jarvis, M. J., & McLure, R. J. 2006, MNRAS, 369, 182
Kaspi, S. 2007, arXiv:0705.1722
Kaspi, S., Brandt, W. N., Maoz, D., Netzer, H., Schneider, D. P., & Shemmer, O. 2007, ApJ, 659, 997
Kaspi, S., Smith, P. S., Netzer, H., Maoz, D., Jannuzi, B. T., & Giveon, U. 2000, ApJ, 533, 631
Kawakatu, N., Anabuki, N., Nagao, T., Umemura, M., & Nakagawa, T. 2006, ApJ, 637, 104
Kawakatu, N., Andreani, P., Granato, G. L., & Danese, L. 2007a, ApJ, 663, 924
Kawakatu, N., Imanishi, M., & Nagao, T. 2007b, ApJ, 661, 660
King, A. 2003, ApJ, 596, L27
King, A. 2005, ApJ, 635, L121
Kollmeier, J. A., et al. 2006, ApJ, 648, 128
Kormendy, J., & Richstone, D. 1995, ARA&A, 33, 581
Kovács, A., Chapman, S. C., Dowell, C. D., Blain, A. W., Ivison, R. J., Smail, I., & Phillips, T. G. 2006, ApJ, 650, 592
Lauer, T. R., Tremaine, S., Richstone, D., & Faber, S. M. 2007, ApJ, 670, 249
Lutz, D., Valiante, E., Sturm, E., Genzel, R., Tacconi, L. J., Lehnert, M. D., Sternberg, A., & Baker, A. J. 2005, ApJ, 625, L83
Magorrian, J., et al. 1998, AJ, 115, 2285
Mainieri, V., et al. 2005, MNRAS, 356, 1571
Manners, J. C., et al. 2003, MNRAS, 343, 293
Maraston, C. 2005, MNRAS, 362, 799
Marconi, A., & Hunt, L. K. 2003, ApJ, 589, L21
Marconi, A., Risaliti, G., Gilli, R., Hunt, L. K., Maiolino, R., & Salvati, M. 2004, MNRAS, 351, 169
Markwardt, C. B., Tueller, J., Skinner, G. K., Gehrels, N., Barthelmy, S. D., & Mushotzky, R. F. 2005, ApJ, 633, L77
Matt, G., Fabian, A. C., Guainazzi, M., Iwasawa, K., Bassani, L., & Malaguti, G. 2000, MNRAS, 318, 173
Matt, G., et al. 1997, A&A, 325, L13
McLure, R. J., & Dunlop, J. S. 2002, MNRAS, 331, 795
McLure, R. J., & Dunlop, J. S. 2004, MNRAS, 352, 1390
McLure, R. J., Jarvis, M. J., Targett, T. A., Dunlop, J. S., & Best, P. N. 2006, MNRAS, 368, 1395
Menéndez-Delmestre, K., et al. 2007, ApJ, 655, L65
Mushotzky, R. F., Cowie, L. L., Barger, A. J., & Arnaud, K. A. 2000, Nature, 404, 459
Mushotzky, R. F., Done, C., & Pounds, K. A. 1993, ARA&A, 31, 717
Nelan, J. E., Smith, R. J., Hudson, M. J., Wegner, G. A., Lucey, J. R., Moore, S. A. W., Quinney, S. J., & Suntzeff, N. B. 2005, ApJ, 632, 137
O'Dea, C. P., De Vries, W. H., Worrall, D. M., Baum, S. A., & Koekemoer, A. 2000, AJ, 119, 478
Ogasaka, Y., Inoue, H., Brandt, W. N., Fabian, A. C., Kii, T., Nakagawa, T., Fujimoto, R., & Otani, C. 1997, PASJ, 49, 179
Osterbrock, D. E. 1977, ApJ, 215, 733
Osterbrock, D. E. 1989, Astrophysics of Gaseous Nebulae and Active Galactic Nuclei (Mill Valley, CA: University Science Books)
Ozawa, H., et al. 2006, Proc. SPIE, 6266, 77
Page, M. J., Stevens, J. A., Ivison, R. J., & Carrera, F. J. 2004, ApJ, 611, L85
Page, M. J., Stevens, J. A., Mittaz, J. P. D., & Carrera, F. J. 2001, Science, 294, 2516
Panter, B., Jimenez, R., Heavens, A. F., & Charlot, S. 2007, MNRAS, 378, 1550
Papovich, C., et al. 2006, ApJ, 640, 92
Parmar, A. N., et al. 2006, Proc. SPIE, 6266, 50
Peng, C. Y., Impey, C. D., Rix, H.-W., Kochanek, C. S., Keeton, C. R., Falco, E. E., Lehár, J., & McLeod, B. A. 2006, ApJ, 649, 616
Peterson, B. M., & Wandel, A. 1999, ApJ, 521, L95
Peterson, B. M., & Wandel, A. 2000, ApJ, 540, L13
Peterson, B. M., et al. 2004, ApJ, 613, 682
Pinkney, J., et al. 2003, ApJ, 596, 903
Polletta, M. d. C., et al. 2006, ApJ, 642, 673
Pope, A., et al. 2006, MNRAS, 370, 1185
Pope, A., et al. 2008, ApJ, 675, 1171
Priddey, R. S., Isaak, K. G., McMahon, R. G., & Omont, A. 2003, MNRAS, 339, 1183
Ptak, A., Heckman, T., Levenson, N. A., Weaver, K., & Strickland, D. 2003, ApJ, 592, 782
Rees, M. J. 1984, ARA&A, 22, 471
Sanders, D. B., Mazzarella, J. M., Kim, D.-C., Surace, J. A., & Soifer, B. T. 2003, AJ, 126, 1607
Sanders, D. B., & Mirabel, I. F. 1996, ARA&A, 34, 749
Sanders, D. B., Soifer, B. T., Elias, J. H., Madore, B. F., Matthews, K., Neugebauer, G., & Scoville, N. Z. 1988, ApJ, 325, 74
Sarzi, M., Rix, H.-W., Shields, J. C., Rudnick, G., Ho, L. C., McIntosh, D. H., Filippenko, A. V., & Sargent, W. L. W. 2001, ApJ, 550, 65
Schneider, D. P., et al. 2003, AJ, 126, 2579
Scott, S. E., et al. 2002, MNRAS, 331, 817
Severgnini, P., Risaliti, G., Marconi, A., Maiolino, R., & Salvati, M. 2001, A&A, 368, 44
Seymour, N., et al. 2007, ApJS, 171, 353
Shields, G. A., Gebhardt, K., Salviander, S., Wills, B. J., Xie, B., Brotherton, M. S., Yuan, J., & Dietrich, M. 2003, ApJ, 583, 124
Shields, G. A., Menezes, K. L., Massart, C. A., & Vanden Bout, P. 2006, ApJ, 641, 683
Silk, J., & Rees, M. J. 1998, A&A, 331, L1
Smail, I., Ivison, R. J., & Blain, A. W. 1997, ApJ, 490, L5
Smail, I., Ivison, R. J., Blain, A. W., & Kneib, J.-P. 1998, ApJ, 507, L21
Smail, I., Ivison, R. J., Blain, A. W., & Kneib, J.-P. 2002, MNRAS, 331, 495
Smith, D. A., & Done, C. 1996, MNRAS, 280, 355
Soltan, A. 1982, MNRAS, 200, 115
Springel, V., Di Matteo, T., & Hernquist, L. 2005, MNRAS, 361, 776
Stevens, J. A., Page, M. J., Ivison, R. J., Carrera, F. J., Mittaz, J. P. D., Smail, I., & McHardy, I. M. 2005, MNRAS, 360, 610
Swinbank, A. M., Chapman, S. C., Smail, I., Lindner, C., Borys, C., Blain, A. W., Ivison, R. J., & Lewis, G. F. 2006, MNRAS, 371, 465
Swinbank, A. M., Smail, I., Chapman, S. C., Blain, A. W., Ivison, R. J., & Keel, W. C. 2004, ApJ, 617, 64
Tacconi, L. J., et al. 2006, ApJ, 640, 228
Takata, T., Sekiguchi, K., Smail, I., Chapman, S. C., Geach, J. E., Swinbank, A. M., Blain, A., & Ivison, R. J. 2006, ApJ, 651, 713
Tremaine, S., et al. 2002, ApJ, 574, 740
Treu, T., Malkan, M. A., & Blandford, R. D. 2004, ApJ, 615, L97
Treu, T., Woo, J.-H., Malkan, M. A., & Blandford, R. D. 2007, ApJ, 667, 117
Valiante, E., Lutz, D., Sturm, E., Genzel, R., Tacconi, L. J., Lehnert, M. D., & Baker, A. J. 2007, ApJ, 660, 1060
Vasudevan, R. V., & Fabian, A. C. 2007, MNRAS, 381, 1235
Veilleux, S., Kim, D.-C., & Sanders, D. B. 1999, ApJ, 522, 113
Veilleux, S., Kim, D.-C., & Sanders, D. B. 2002, ApJS, 143, 315
Veilleux, S., Sanders, D. B., & Kim, D.-C. 1997, ApJ, 484, 92
Vestergaard, M. 2002, ApJ, 571, 733
Vestergaard, M. 2004, ApJ, 601, 676
Vestergaard, M., & Peterson, B. M. 2006, ApJ, 641, 689
Vignati, P., et al. 1999, A&A, 349, L57
Wandel, A., Peterson, B. M., & Malkan, M. A. 1999, ApJ, 526, 579
Wang, W.-H., Cowie, L. L., & Barger, A. J. 2004, ApJ, 613, 655
Ward, M. J., Done, C., Fabian, A. C., Tennant, A. F., & Shafer, R. A. 1988, ApJ, 324, 767
Ward, M. J., Geballe, T., Smith, M., Wade, R., & Williams, P. 1987, ApJ, 316, 138
Webb, T. M., et al. 2003, ApJ, 587, 41
White, N. E., Tananbaum, H., Weaver, K., Petre, R., & Bookbinder, J. A. 2004, Proc. SPIE, 5488, 382
Whittle, M. 1985, MNRAS, 213, 33
Whittle, M., Pedlar, A., Meurs, E. J. A., Unger, S. W., Axon, D. J., & Ward, M. J. 1988, ApJ, 326, 125
Willott, C. J., McLure, R. J., & Jarvis, M. J. 2003, ApJ, 587, L15
Wootten, A. 2006, ASP Conf. Ser. 356, Revealing the Molecular Universe: One Antenna is Never Enough (San Francisco, CA: ASP), 59
Wyithe, J. S. B., & Loeb, A. 2003, ApJ, 595, 614
Young, S., Hough, J. H., Efstathiou, A., Wills, B. J., Bailey, J. A., Ward, M. J., & Axon, D. J. 1996, MNRAS, 281, 1206
Yu, Q., & Tremaine, S. 2002, MNRAS, 335, 965